

THE MAGNETIC FIELD STRUCTURE AND ITS VARIATIONS  
IN THE SOLAR FLARE REGION 24

BY

[S. I. Gopasyuk, M. B. Ogir',  
B. Severnyy, and Ye. F. Shaposhnikova]

GPO PRICE \$  
CFSTI PRICE(S) \$  
Hard copy (HC) \$3.00  
Microfiche (MF) 175

N 653 July 65

MICROFILM FORM 502

N66 27189

(ACCESSION NUMBER)

83

(PAGES)

(NASA CR OR TMX OR AD NUMBER)

(THRU)

(CODE)

29

(CATEGORY)

Translation of: *Struktura magnitnykh poley i yeye izmeneniya v rayone solnechnykh vspyshek*  
Akademiya Nauk SSSR, Izvestiya Krymskoy Astrofizicheskoy Observatorii, Vol. XXIX, pp. 15-67, 1963.

*comp. auth.* NATIONAL AERONAUTICS AND SPACE ADMINISTRATION,  
WASHINGTON, D.C.

APRIL 1964 83 p refs

NASA TT F-8724

Transl. into ENGLISH  
from Inv. Krymsk.  
Astrofiz. Observ.  
(Moscow), v. 29,  
1963 p 15-67

→ Umc.

[From: Akademiya Nauk SSSR, Izvestiya Krymskoy Astrofizicheskoy Observatorii,  
Vol. XXIX, 1963, pages 15 - 67]

# THE MAGNETIC FIELD STRUCTURE AND ITS VARIATIONS IN THE SOLAR FLARE REGION

by S. I. Gopasyuk, M. B. Ogir', A.B. Severnyy and Ye. F. Shaposhnikova

13602

4

In 51 cases a study has been made of the configurations and magnetic fields in spot groups, before and after a flare, for 4 classes of flares. Class I - proton flares of importance 3 and 3+, which were responsible for a cosmic ray increase effect recorded on balloons. Flares producing this effect at ground level are included in this class. Class II - proton flares of importance 3 and 3+. No effect was recorded on balloons, but the flares were responsible for absorption in the polar cap. Class III - flares of importance 3 and 2+. No geophysical effects. Class IV - flares of importance 2 and 2+.

Considerable changes in the configurations of spots have been noted after intense flares (class I and partly class II). The configuration widens, one of the spots with similar polarity is pushed out. The possibility of producing laboratory models of field of spot configurations is shown. For each of the 51 cases a model of the field before and after the flare has been constructed. It is found that the transversal field gradient in neutral points of the configurations-models decrease very sharply after flares of classes I and II. For flares of class III and IV this decrease is essentially smaller (tables 7 - 10 and figs. 6 and 7).

Results of modeling show that there is a correlation between the importance of the flare and the gradient before the flare: the greater the importance of the flare, the larger the gradient. No flare of importance 3 has been observed with a gradient less than 0.1 gs/km and no flare of importance 2 with a gradient exceeding this value. These results are confirmed in several cases by a comparison of the magnetic charts, obtained before and after a flare, with the magnetograph. For example the field gradient after the flares of August 22, 1958, July 16, 1959 and August 18, 1959 showed an essential appreciable decrease in most of the directions linking the poles-spots. An increase of the field gradient immediately before a flare is noted. *Author*

## INTRODUCTION

The purpose of this work is find out in what spot configurations, magnetic field carriers, do the flares originate, and what variations of the magnetic field configurations are associated with them. Of particular interest is the problem of whether the power of the flare and such of its effects as the radiation of cosmic rays and protons, which produce absorption in the



polar cap, are connected with the characteristic features of the field configurations or its variations. In the study of this problem we are trying to utilize all the available information obtained during the IGY on the magnetic fields of the groups of spots in which flares of various strength had occurred (Part 1). In order to simplify the large amount of calculation work, and because of the lack of information on transverse fields, all the data on the absolute magnetic field voltages in the groups were used for the construction of laboratory models of field configurations similar to the solar ones. With these models, we succeeded in studying a number of important characteristics of field configurations connected with the flares (Part 2). These results could be confirmed by the use of magnetic charts produced on a magnetograph whenever recordings were available of the fields before and after the flares (Part 3).

Part 1 of this work was prepared and written by M. B. Ogir' and Ye. F. Shaposhnikova, Part 2 by A. B. Severnyy and Part 3 by S. I. Gopasyuk.

## 1. OBSERVATION DATA

Under consideration are powerful flares of two points and higher. All the flares are divided into four classes: I - powerful 3 and 3+ point flares accompanied by increasing intensity of cosmic rays on wide latitudes which were recorded by means of ordinary and sounding balloons (this includes, of course, the flares which increased the intensity of the cosmic rays at the Earth level); II - powerful 3 and 3+ point flares producing an absorption in the ionosphere at high latitudes (polar block-outs and increase in  $f_{min}$ ) for which no effect had been observed in the cosmic rays or no such measurements had been

made; III - powerful 3 and 2+ flares which definitely showed no recorded increase in cosmic radiation on Earth; IV - 2 and 2+ point flares not accompanied by any recorded effects of cosmic radiation or geophysical effects.

The flares with a heliographic longitude ( $\lambda$ ) over  $60^\circ$  were excluded with a view to obtaining more authentic results. Taken out of consideration also were the flares without adequately defined magnetic fields (in case the magnetic fields were determined only on the large spots or only on parts of the visible disc, because of weather conditions); the flares observed before the IGY were entirely eliminated for the same reason.

The configuration of the group of spots and their magnetic fields during the passage of a given group over the visible solar disc was examined in the case of each flare. The magnetic fields and positions of the spots were selected in such a way as to be closest to the beginning and end of the flare but not to coincide with the flare itself. Occasionally, the position of the spots selected was based on the observations of one observatory, and the magnetic fields on the observations of another. Whenever the magnetic observations of one observatory, closest to the beginning or end of the flare, were not complete enough, they had to be supplemented with observations of other observatories as close to the flare in point of time as possible. It should be pointed out that it was not always possible to select the magnetic fields and positions of the spots several hours before the beginning or after the end of the flare. In a number of cases the time gap between the observations of the magnetic fields and the flares amounted to 24 hours or even longer (see the sketch drawings of the groups in Figs. 1-4).

The position of the flares in this configuration of the spots was determined by the coordinates taken from the catalogs listed below. It should be pointed out that the accuracy of pinpointing the flare is not very high. The main reason for this is that we still do not have a uniform system or rules for determining the flare coordinates. That is why the flare coordinates estimated by different observatories frequently show a difference of several degrees. This discrepancy in the evaluation of the flare coordinates depends a great deal on the nature of the flares: it is not very large in the case of "static" flares [1], but it can reach a very large magnitude in the case of "dynamic" flares [1]. The coordinates of the "dynamic" flares estimated by some observatories usually characterize the beginning of the flare, that is they are close to the true source of the flare, whereas the majority of the observatories usually indicate the coordinates of the center of the flare in the stage of its maximum development.

An additional check-up, as described below, was made for the purpose of eliminating the inaccuracy in determining the location of the flare during the selection of the spot configuration in which the flare originated. Whenever it was possible to select two or more close determinations of the position of the spots before a powerful flare (or after the end of a flare), and if not considerable flares (higher than point one) were observable in that period, the follow pattern could be observed: before the flare, the nearby spots (or the nuclei of some multipolar spot) gradually drew closer together, but after the flare the spots (nuclei) of similar polarity are visibly repulsed (see Part 2 below). These changes in the location of the spots

(nuclei) were observed only in the same places as the flares. It was this circumstance that facilitated the confident selection of the spot configuration (or the nuclei in the case of a multipolar spot) where the flare originated.

The following sources of information were used in this experiment:

1. The E. Dodson and R. Hedeman catalogs for 1957-1959 [2].
2. The quarterly bulletins of solar activity No. 119-128 for 1957-1959 [3].
3. Information of the world center of solar activity No. 13-15 for 1957-1961 [4].
4. Solar maps of the Fraunhofer institute for 1957-1961 [5].
5. The catalog of magnetic fields of the sun spots during the IGY (1 July 1957 - 31 December 1958) [6].
6. A list of proton bursts for 1957-1961 [7].
7. Diagrams containing information on geophysical effects and type IV radio flashes produced by chromospheric flares [8].
8. A combined list of flares bases on balloon measurements observed mostly by A. N. Charakhchyan\* [9].
9. Motion pictures of flares taken with a KG-1 (Nauchnyy) and AFR-2 (Simeiz) coronagraph for 1957-1961.
10. Photoheliograms received by a BST (Nauchnyy) and AFR-2 (Simeiz, Pirkuli, Kislovodsk) in the period of 1957-1961.
11. Spectroheliograms and magnetograms received by BST (Nauchnyy) for 1957-1961.

---

\* A. N. Charakhchyan kindly made that list available to us.

12. Information obtained in the observations of the magnetic fields by Soviet observatories (the Crimean Astrophysical Observatory, the Main Astronomic Observatory, Kislovodsk, Ismiran) for 1959-1961.

### A Description of Various Classes of Bursts

#### I. Radiosonde-Measured Proton Bursts

This class includes all the proton bursts for which radiosonde measurements are available according to list [9]. Included also are the powerful proton bursts for which there were no radiosonde measurements but which were geophysically close to the flares that had produced cosmic rays in the stratosphere according to measured intensity (some of the observations of the flares had been made before the beginning of the radiosonde measurements). The data on the geophysical effects of these flares as well as the class II flares are not cited in this article. A detailed description of these phenomena appears in article [7].

Table 1

No.	Date	Intensity points	Observation time		Coordinates		Remarks
			beginning	end			
1	3.VII 1957	3+	07 <sup>h</sup> 12 <sup>m</sup>	11 <sup>h</sup> 45 <sup>m</sup>	N 14	W 40	No radiosonde measurements Ditto "
2	28.VIII	3	08 10	14 04	N 10	W 42	
3	20.X	3+	16 37	18 04D	S 31	E 33	
					S 26	W 45	No radiosonde measurement
					S 26	W 35	
4	7.VII 1958	3+	00 20	04 14	N 24	W 08	
5	16.VIII	3+	04 33	08 31	N 14	W 50	
6	22.VIII	3	14 17	17 17D	N 18	W 10	
7	10.VII 1959	3+	02 10E	10 03D	N 22	E 64	
8	14.VII	3+	03 25E	11 21	N 17	E 06	
9	16.VII	3+	21 14	24 30	N 16	W 30	
10	1.IV 1960	3+	08 40	13 20	N 12	W 11	
11	12.XI	3+	13 25	19 22	N 26	W 05	
12	15.XI	3	02 07	04 27	N 26	W 35	
13	28.IX 1961	3	22 02	01 30	N 12	E 29	

Note. E means that the actual beginning of the flare occurred before the indicated time (before the beginning of the observations); D means that by the end of the observations the flare was still on.

The time indicated in this article is always universal time.

In view of the particular importance of the proton bursts, we provide a detailed description of the groups of spots in which each of the flares occurred, as well as the sketches of these spot groups and their magnetic fields before and after the flares with an indication of the observatory producing the information and the average time of the occurrence, correct to 0.01 part of a day. If the average moments of determining the position of the spots and the magnetic fields do not coincide, two different moments are indicated on the sketches, the first of them applying to the determination of the spot position and the second to the magnetic fields.

As pointed out earlier, whenever detailed observations of the fields were lacking, the data on such fields required in connection with some of the spots were taken from the observations of other laboratories on that particular day or even on the nearest days. Several such uncertain determinations are shown on the sketches in circles which also contain an indication of the observatory which determined the magnetic field, and the average moment of its determination. The intensity and polarity of the spots whose position is closely associated with that of the flare are underscored with a straight line on the sketches. The names of the observatories are abbreviated as follows: Cr -- Crimean Astrophysical Observatory, MW -- Mount Wilson Observatory, Pots -- Potsdam Observatory, Pulk -- Main Astronomical Observatory (Pulkovo), K -- Kislovodsk mountain station, and I -- Izmiran.

The diameter of the sun's representation on which the sketch is based is indicated in each case. The approximate position of the flare on the sketch is indicated by a slanted cross. During the IGY the numeration of the groups

was based on the system of the Mount Wilson observatory. The numbers of the groups are not indicated in connection with the other flares. We will now describe the individual flares.

The flare of July 3, 1957, originated in the spot group 12,434. The group appeared from behind the fringe of the sun and was first observed on 24 June. It consisted of one large spot and a number of small ones. The number of the small spots and their size was steadily decreasing as the group kept moving toward the western fringe of the sun. The flare occurred near the large spot which had three powerful nuclei of various polarity in its penumbra. There were two major centers and several small ones in the flare. These centers did not originate simultaneously: the first flare occurred in the eastern part (7 12), and after a while a new flare center appeared in the western part (8<sup>h</sup> 30<sup>m</sup>). The magnetic fields nearest to the beginning of the flare were determined by the Potsdam observatory on 3 and 27 July, but unfortunately it determined only the polarity without any indication of the intensity. That is why the position of the spots was based on the determination made by the mentioned observatory but the position of the magnetic fields was plotted on the basis of the determinations made by the Crimean Astrophysical observatory on 3 and 19 July (the position of the spots for that moment had not been indicated). The nearest determination of the magnetic fields made by the Mount Wilson observatory 3<sup>d</sup>, 56 July was used after the flare. As a result of the flare the intensities of all the powerful poles were reduced, and the spots diverged to some extent (see sketch in Fig. 6). The flare of 3 July was observed by our observatory, and is discussed in detail in [10, 11]. That flare was also observed by numerous observatories in the world, and a detailed description of it appears in [12, 13].

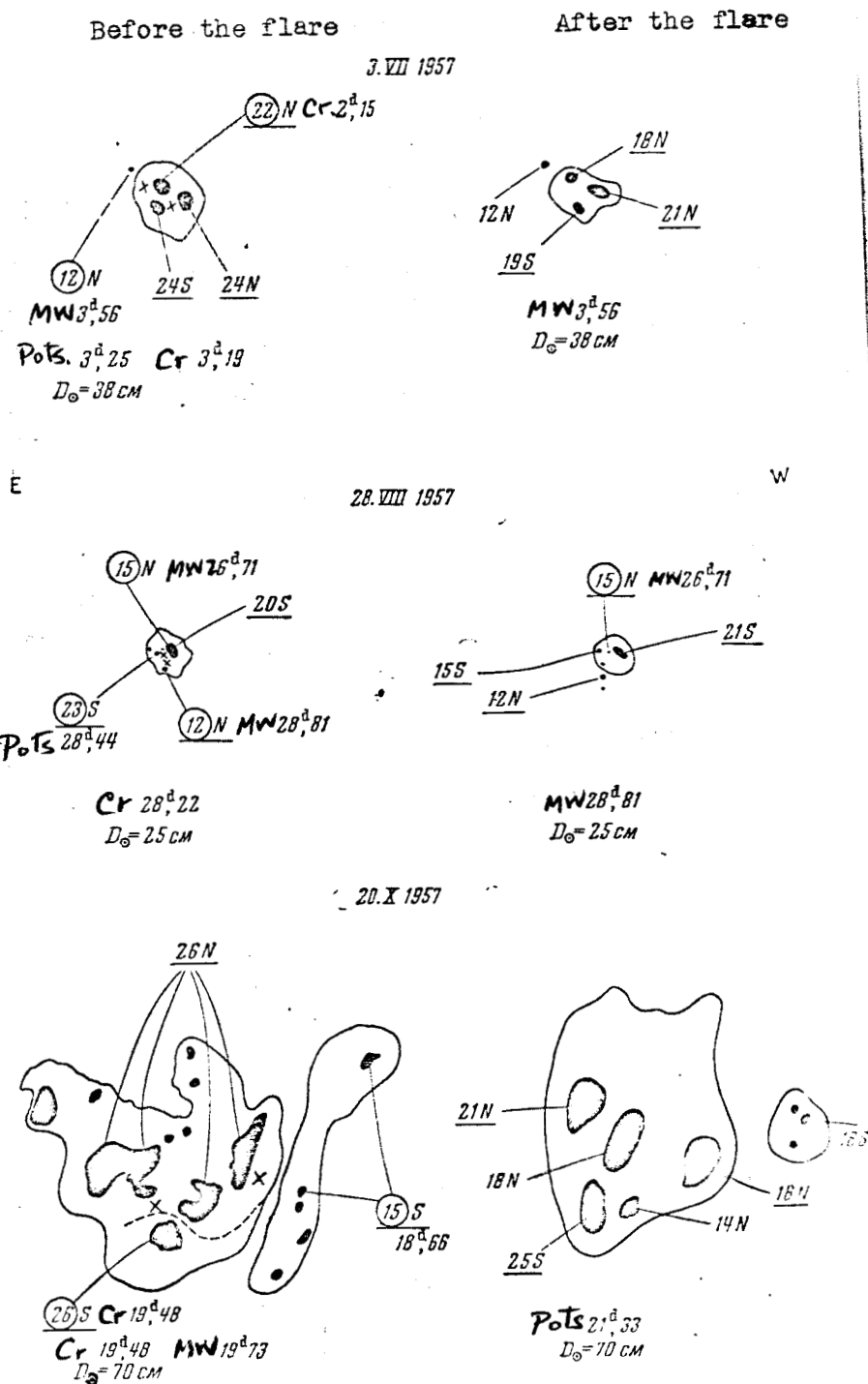
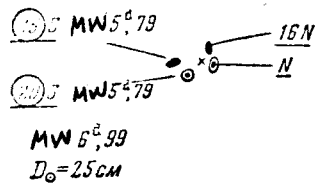


Fig. 1. Configuration of the spots and their magnetic fields in Class I bursts

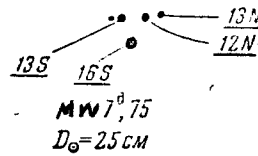
(see also pp. 10, 11 and 12)

Before the flare

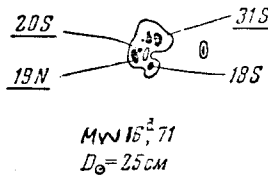
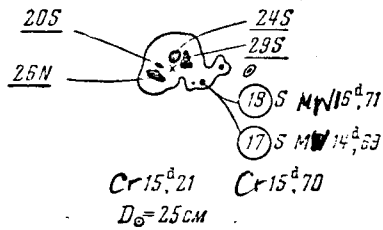
7. VII 1958



After the flare



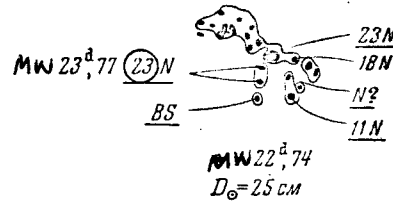
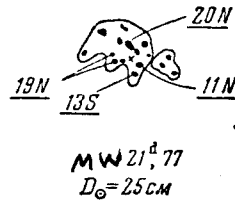
16. VIII 1958



E

W

22. VIII 1958



10. VII 1959

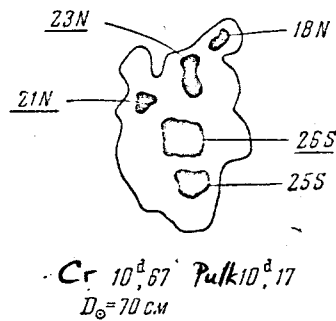
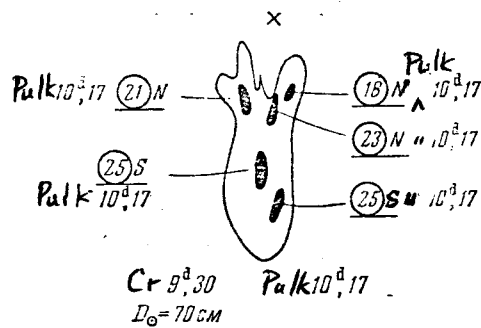


Fig. 1. Continued

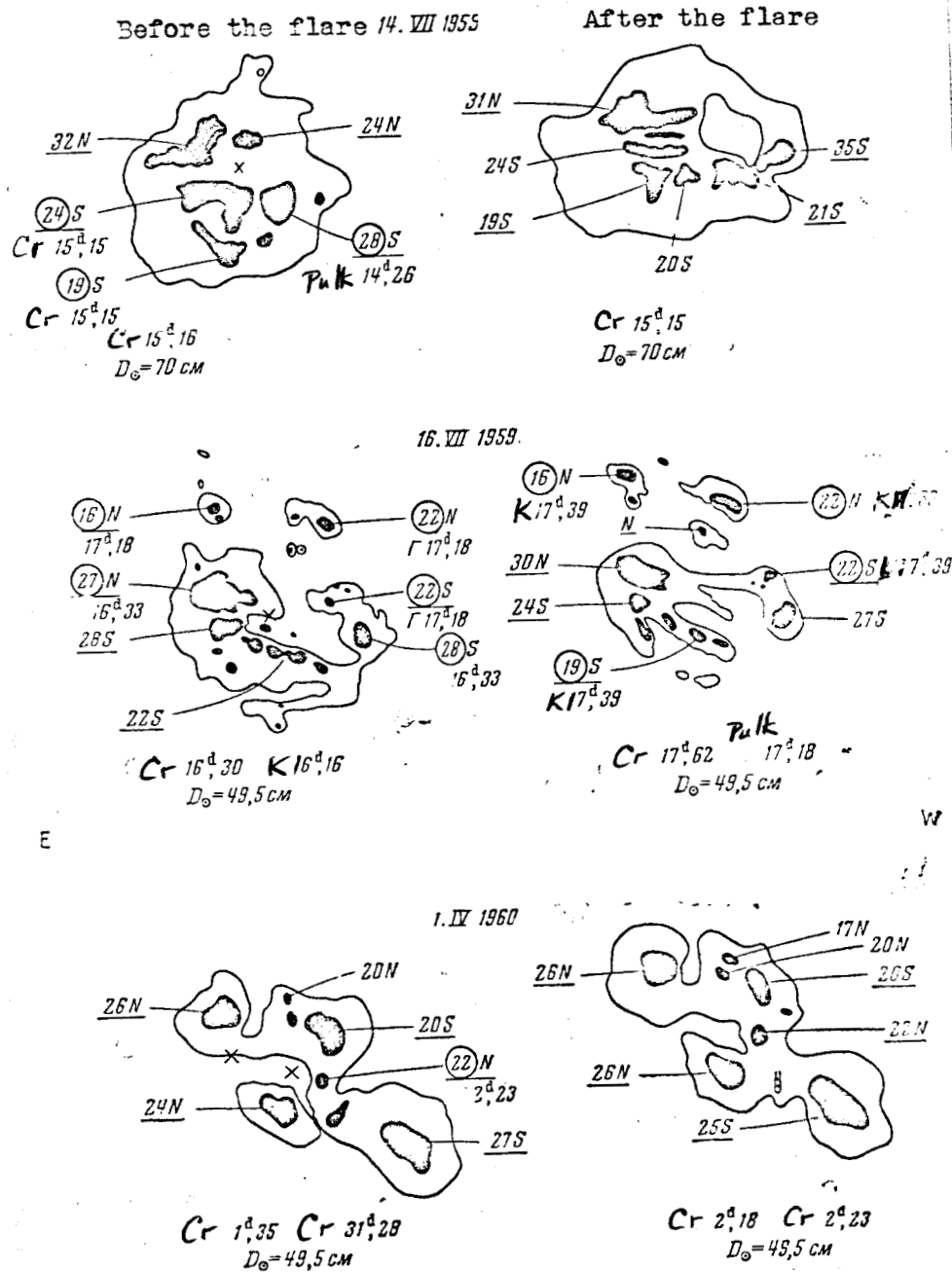


Fig. 1. Continued

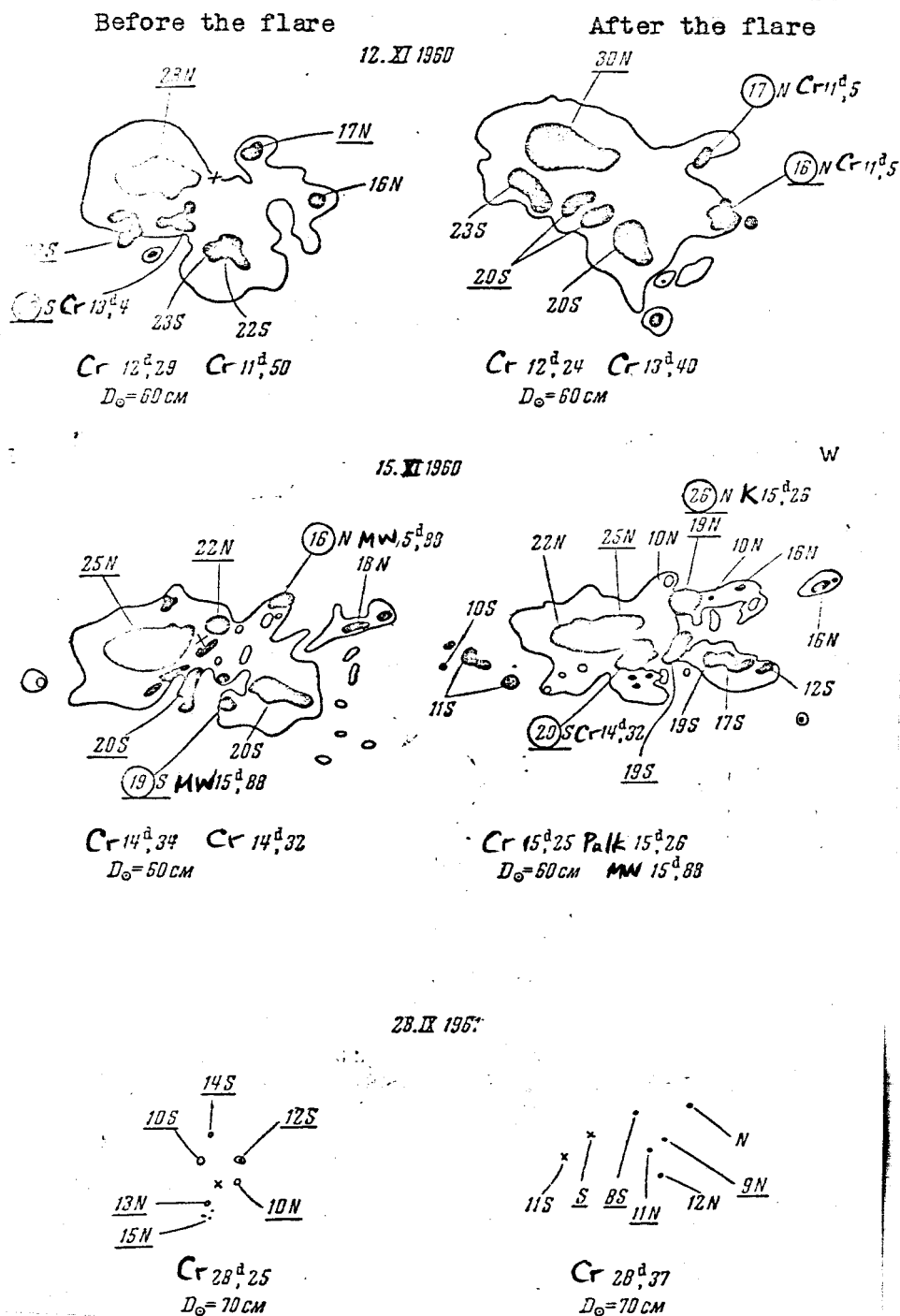


Fig. 1. End

The flare of 28 August 1957 occurred in the group of spots 12,579. That group emerged from behind the edge of the sun in the form of two spots interconnected by a fairly narrow penumbra isthmus. By the end of 27 August the spots were already separated (see observations of Mount Wilson observatory 27<sup>d</sup>, 31 August). The proton burst occurred in the southern (tail) spot of the group which had several nuclei of various polarity in its penumbra. There were two major centers in the flare that had originated simultaneously but reached their maximum intensity at different times. The magnetic fields determined by the Crimean and Potsdam observatories were found to be closest to the beginning of the flare in point of time. The position of the spots was taken from the determination of the Crimean observatory of 28 and 30 August. So were the magnetic fields of that moment which were supplemented by the observations of the Potsdam and Mount Wilson observatories. Attention should be called to the fact that the determination of the magnetic field of the 15 N pole was taken from the observations of the Mount Wilson observatory 26<sup>d</sup>, 31 August. That pole was observed on 27 and 28 August, but its magnetic field was not determined. The Mount Wilson observatory, which provides the most detailed descriptions of magnetic fields, made no observations on 27 August, and failed to determine the magnetic field of the mentioned pole on 28 August. After the flare it was found that one of the poles (12 N) had been pushed out of the general spot penumbra (see sketch and Fig. 6). The flare was observed in our laboratory and described in detail in [10].

The flare of 20 October 1957 occurred in the group of spots 12,689. The group appeared on 11 October from behind the edge. It was a group of large

and well developed spots. The flare originated in the large tail spot which had nuclei of various polarity in its penumbra. Two centers originating at different times were observed in the flare: the western center appeared first and was followed by the eastern a few minutes later. As a result of the flare, the intensities of the N-polarity poles were greatly reduced.

The flare of 7 July 1958 originated in the group of spots 13,350. The group appeared on 29 June from behind the edge in the form of several spots which had already been in a stage of disintegration. The flare originated between the small spots in the central part of the group. As a result of the flare, the 16 N pole (determined by the Mount Wilson Observatory 6<sup>d</sup>, 99 July) was divided into two poles with intensities of 13 and 12 N (determined by the Mount Wilson Observatory 7<sup>d</sup>, 75 July). The S-polarity poles were slightly reduced in point of intensity, and the distance between them was considerably increased (see sketches and Fig. 6).

The flare of 16 August 1958 originated in the group 13,434. The group appeared on 6 August from behind the edge. Heading that group was a large spot surrounded by small spots, and its tail part consisted of small spots. The flare occurred in the large spot which contained nuclei of various polarity in its penumbra. The flare caused a rupture of the penumbra of the spot at the place of the outburst.

The flare of 22 August 1958 occurred in the group 13,464. The group appeared from behind the edge on 15 August. It had a complex structure: on 22 August it consisted of a large spot in the central part of the group and smaller spots in the head and tail parts. A class II proton burst was observed

on 20 August in the head part of that group causing the disintegration of the head spot (see description in section on class II flares). The flare of 22 August originated in the large spot in the central part of the group containing nuclei of various polarity in its penumbra. As a result of the flare, the large spot broke up into several smaller spots. It should be pointed out that another class II proton burst was observed in the same group on 26 August (see description of flare in section on class II flares). The flare was observed in our observatory and described in detail in [14, 15].

The flares of 10, 14 and 16 July 1959 occurred in the same huge multipolar spot consisting of several large nuclei. The group appeared from behind the edge on 9 July. While passing over the visible disc of the sun it produced 11 powerful flares of points  $\geq 2$  and a very large number of less intensive flares. The flare of 10 July 1959 occurred near the nuclei of the northern polarity. It is quite difficult to estimate the changes occurring in the group after that flare as the group was close to the edge at that time. A study of that group in the following days revealed that the nuclei of the southern polarity in it was gradually breaking up and the westernmost nucleus among the nuclei of the southern polarity moved off to the west gradually leaving the general penumbra.

As a result of the flare on 14 July 1959 which occurred approximately in the center of the group but a little closer to the nuclei of the southern polarity, the 28 S nucleus was almost completely pushed out of the general penumbra. A large nucleus 21 S came into being to the east of that nucleus after the flare. The latter was observed in our observatory and described in

detail in [16, 17].

The flare of 16 July 1959 also occurred approximately in the center of the group under consideration. After the flare, the nuclei 22 S and 28 S visibly shifted from the nuclei 27 N and 28 S which were to the east of them (see sketch and Fig. 6). The nuclei in the group broke up and scattered from the general penumbra. The flare was observed at the Mount Wilson Observatory and described in [18, 19].

The flare of 1 April 1960 occurred in a very well developed and large group of spots of various polarity with a very high field intensity. That group originated on the solar disc on 26 March in the form of small pores. On 27 March the group already included one large spot and several small ones within the general penumbra. The development of that group was extremely rapid. On 28 March it consisted of a large spot with two large nuclei in the general penumbra. The number of nuclei in the penumbra increased in the following days. The general penumbra in the nuclei gradually acquired a very disconnected form, and the nuclei were divided into four fairly stable groups with isthmuses between their penumbras. By 1 April these nuclei grew very large in size. A picture of the evolution of that group is presented in [20]; it is also pointed out there that the group was characterized by great activity and produced powerful geophysical and radio effects. It is pointed out in [20] that the group is anomalous in its development, according to its geometrical configuration intrinsic movements and magnetic polarities. The flare of 1 April occurred in the center of the group under consideration. Unlike all the other class I flares, it was not followed by any noticeable changes in the group of spots, so that it can be considered anomalous also in this respect. That flare

was observed also in our observatory.

The flares of 12 and 15 November 1960 occurred in the extensive and very well developed group of large spots appearing at the edge on 6 November. All the nuclei of that huge group were in the general penumbra. Considerable changes were taking place among the spots of the southern polarity as the group moved across the visible disc of the sun. The large western nucleus was gradually moving away from the fairly stable nucleus of northern polarity and new nuclei of southern polarity came into being between them.

The flare of 12 November 1960 occurred in the multipolar rail part of the group with a high intensity near the spots 17 N and 28 N. After the flare the 17 N nucleus moved far from the 28 N nucleus (see sketch and Fig. 6).

The flare of 15 November 1960 also occurred in the tail part of the group. After the flare the 25 and 22 N nuclei moved farther apart and the 25 N and 20 S nuclei drew closer together (see sketch and Fig. 6), and the 20 S nucleus revealed a considerable increase in size. The flares of 12 and 15 November are described in detail in [19].

The flare of 28 September 1961 occurred in a group that had appeared from behind the edge of the Solar disc on 25 September. The group consisted of several large spots in the head part and a number of small spots in the tail. The flare occurred in the tail part among the small spots with a low magnetic field intensity. After the flare the pole 12 S was pushed out of the spot with two nuclei of different polarity (10 N and 12 S) in the general penumbra. But the nuclei of northern polarity located near the spot of the flare drew closer to each other, particularly the 13 N and 10 N. On the day

after the flare the spots in the tail part of the group were considerably reduced in size and their field intensity grew weaker.

## II. Proton Flares Without Radiosonde Measurements

These include the flares which are listed as proton bursts in list [7]. The information on this class of flares is given in Table 2. The description of the flares and sketches are based on the same principle as in the class I flares.

Table 2

No.	Date	Intensity points	Observation time		Coordinates
			beginning	end	
1	31.VIII 1957	3	12 <sup>h</sup> 57	14 <sup>h</sup> 55 <sup>m</sup> Д	N 25 W 02
2	3.IX	3	14 12	17 27	N 23 W 30
3	10.IX	3	02 23	03 00Д	N 14 E 16
4	11.IX	3	02 36E	07 28	N 13 W 02
5	21.IX	3	13 30	15 10	N 10 W 06
6	20.VIII 1958	2+	00 42	01 28	N 16 E 18
7	26.VIII	3	00 05	01 24	N 20 W 34
8	18.VIII 1959	3	10 19	13 50	N 11 W 24
9	29.III 1960	2+	06 40	08 52	N 12

The flare of 31 August 1957 occurred in the group 12,580. The group had appeared from behind the edge of the solar disc on 25 August and consisted of large and well developed spots. The proton flare originated in the very large head spot of the group which contained numerous nuclei of different polarities in its penumbra. The closest determination of the magnetic fields, in point of time, was made by the Mount Wilson Observatory 30<sup>d</sup>, 69 August, that

is almost 24 hours (21:30) before the flare, as no observations were made in the morning of 31 August (except by the Mount Wilson Observatory). The magnetic fields after the flare were determined about 1.5 hours later by the Mount Wilson Observatory for 31<sup>d</sup>, 71 August.

After the flare the large head spot disintegrated, and its eastern portion became separated (where the flare occurred). Each of the two poles, 19 N and 19 S (according to the 30 August observations) was divided into two, and the intensity of each pair of poles was the same as of the original poles (19 S was divided into two poles each with an intensity of 19 S), or somewhat lower (19 N was divided into two poles with an intensity of 15 N each). Thus the overall aspect of the magnetic field in the flare area became more complicated rather than simplified.

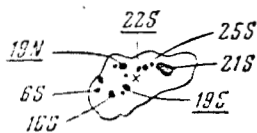
The flare of 3 September 1957 occurred in the same group 12,580 (see description of the group given in connection with flare of 31 August). Between 31 August and 3 September the group was in a stage of disintegration; the complex-structure spots kept breaking up into smaller ones. The proton flare of 3 September occurred in the tail spot which had nuclei of various polarities in its penumbra. The place of the flare is indicated on the map of the Mount Wilson Observatory (which observed that flare) on 3 September. After the flare the tail spot disintegrated (the N and S polarities became separated). The flare was observed by our observatory, and is discussed in detail in [10].

The flare of 10 September 1957 occurred in group 12,596. When the group appeared from behind the edge of the solar disc on 4 September it had already been in a stage of disintegration: it consisted of many irregularly

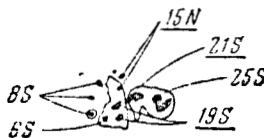
Before the flare

After the flare

31. VIII 1957



MW 30<sup>d</sup>, 59  
D<sub>0</sub> = 25 cm

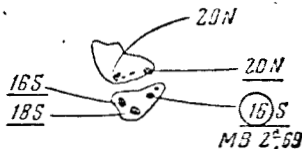


MW 31<sup>d</sup>, 71  
D<sub>0</sub> = 25 cm

3. IX 1957



MW 2<sup>d</sup>, 59  
D<sub>0</sub> = 25 cm



MW 3<sup>d</sup>, 57  
D<sub>0</sub> = 25 cm

E

W

10. IX 1957

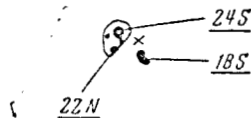


MW 9<sup>d</sup>, 57  
D<sub>0</sub> = 25 cm

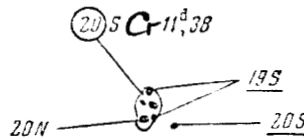


Pots 10<sup>d</sup>, 41  
D<sub>0</sub> = 18 cm

11. IX 1957



MW 10<sup>d</sup>, 80 Cr 10<sup>d</sup>, 56  
D<sub>0</sub> = 25 cm



MW 11<sup>d</sup>, 73  
D<sub>0</sub> = 25 cm

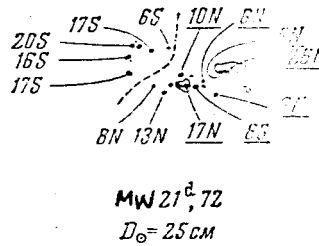
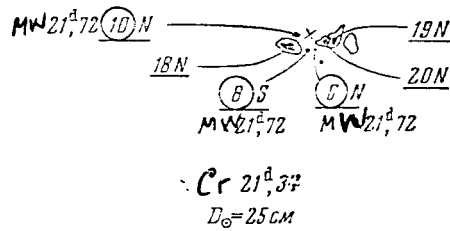
Fig. 2. Configuration of the spots and their magnetic fields involved in Class II flares.

(See also pages 21 and 22)

Before the flare

After the flare

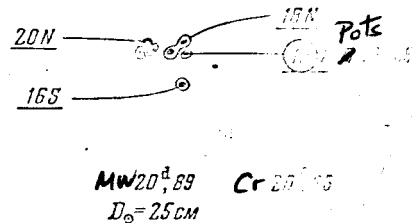
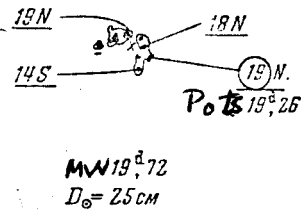
21. IX 1957



E

W

20. VIII 1958



26. VIII 1958

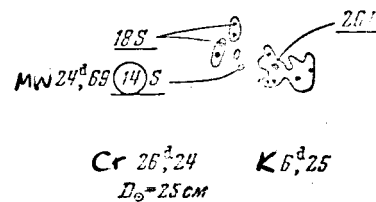
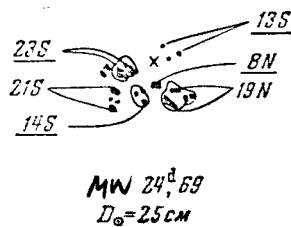
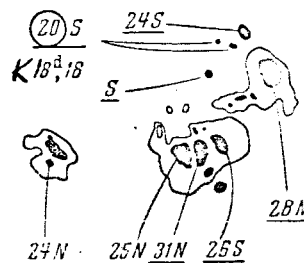
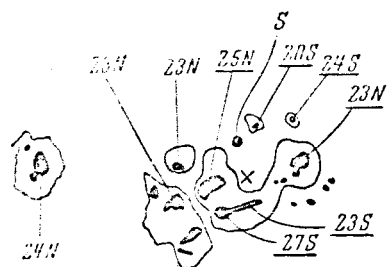


Fig. 2. Continued

Before the flare

After the flare

18. VIII 1959



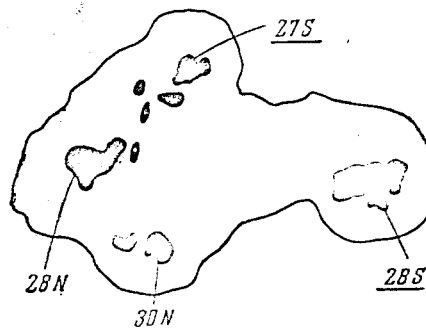
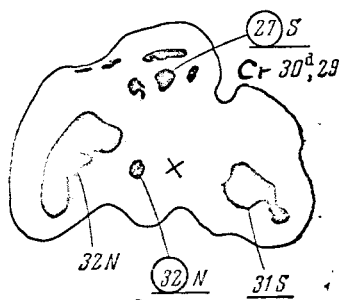
Cr 19<sup>d</sup>, 27 Cr 18<sup>d</sup>, 18  
D<sub>0</sub> = 49,5 cm

Cr 18<sup>d</sup>, 27 Cr 19<sup>d</sup>, 17  
D<sub>0</sub> = 49,5 cm

E

W

29. III 1960



Cr 29<sup>d</sup>, 23 K 29<sup>d</sup>, 19  
D<sub>0</sub> = 80,05 cm

Cr 30<sup>d</sup>, 26 Cr 30<sup>d</sup>, 28  
D<sub>0</sub> = 80,05 cm

Fig. 2. End.

shaped and small spots. The proton flare occurred in the largest spot in the tail end of the group which had nuclei of various polarity in its penumbra. As a result of the flare, the 20 S pole (determined by the Mount Wilson Observatory, 9<sup>d</sup>, 67) was knocked out of the general penumbra, and a small new spot with an 18 S magnetic field (determined by the Potsdam Observatory 10<sup>d</sup>, 41 September) was formed to the west of the tail spot under consideration (see sketches).

The flare was observed by only one station (Sydney).

The flare of 11 September 1957 originated in the same group 12,596 (see description of flare of 10 September). It occurred almost in the same spot (slightly to the west) as the flare of 10 September. As a result of the flare, the 24 S magnetic pole (determined by the Mount Wilson Observatory 10<sup>d</sup>, 80 September) broke up into three poles; the two end poles were determined by the Mount Wilson Observatory as 19 S, and the central one was defined by the Crimean Astrophysical Observatory 11<sup>d</sup>, 38 September as 20 S. Thus the picture of the magnetic fields in the region of the proton flare became complicated. This apparently brought about the two point-two flares of 12 September (7th and 15th hour universal time) in the place of the proton flares of 10 and 11 September. After that, the magnetic fields were reduced.

The flare of 21 September 1957 occurred in the group 12,634. That group had been formed on the solar disc on 19 September in the northeastern quadrant near the central meridian: it was a very small spot. On 20 September that group revealed four small spots, and by 21 September the group had expanded a great deal: it had seven spots of considerable size. The length of the group

in point of longitude on that day was more than  $10^{\circ}$ . The proton flare occurred in the head part of the group between two small spots. No great changes were produced by the flare: the western spot was somewhat increased in size (it merged with the neighboring, particularly the western small spot), and the eastern spot was somewhat decreased.

The flare of 20 August 1958 occurred in the group 13,464. A description of the group is given in connection with the class I flare of 22 August. The proton flare of 20 August originated in the small head spot which contained several nuclei of various polarity in its penumbra. As a result of the flare, the head spot broke up into three small spots. The 14 S and 19 N poles (as determined by the Mount Wilson Observatory 19<sup>d</sup>, 72 August and the Potsdam Observatory 19<sup>d</sup> 26) were knocked out of the general penumbra of the spot (see sketches) and formed new small spots to the west and south of the head spot with 19 N and 16 S fields (on 20 August the Mount Wilson Observatory reported only the position of the spot without determining the polarities; the fields were therefore taken from the report of the Crimean Astrophysical Observatory 20<sup>d</sup>, 23). After the flare, the nuclei of opposite polarity became separated.

The flare of 26 August 1958 originated in the same group 13,464 (see description of the group in the section on class I flares and the previous flare of 20 August). From 20 through 26 August there were three proton flares in the group: on 20 August (class II), 22 August (class I) and 26 August (class II). These powerful flares produced a radical change in the configuration of the group: the large spots broke up into small ones. By 26 August

the group had one medium-size spot in its head, central and tail parts which were connected with numerous small spots. The flare of 26 August occurred in the head part of the group; after the flare, some of the small spots disappeared and the polarities were divided into two separate groups.

The flare of 18 August 1959 occurred in a complex and well developed multipolar group of spots which came up from behind the edge on 8 August. In its movement across the visible portion of the solar disc until 18 August, the group became visibly complicated. The flare of 18 August was the only flare of point-3 intensity occurring in a given group of spots during their passage across the visible portion of the solar disc. There were also two other flares of point-2 intensity and a considerable number of less intensive flares. The flare of 18 August occurred approximately in the center of the group. All the nuclei moved considerably further apart after that flare. Particularly conspicuous was the change in the position of the nucleus 25 N which on 19 August (its intensity rose to 31 N) was located on a straight line with the nuclei 25 N and 26 S. In the days following the flare under consideration, the structure of the given group of spots became simplified. The large central spot consisting of several nuclei became less complex -- the two large nuclei of northern polarity merged into a single nucleus, and two nuclei of varying polarity remained in the general penumbra.

The flare of 29 March 1960 occurred in the same large group of large spots as the flare of 1 April 1960 (see the description of group above). During that flare the group had not yet achieved such a development as by the time of the flare of 1 April 1960, and it consisted of three spots in the

general penumbra. After that flare, all the nuclei moved apart, and the fourth nucleus of the group 30 N was formed (see sketch).

### III. Flare With and Intensity of 3 and 2+ Points Without Cosmic Ray Effects

This involves a collection of flares of the mentioned intensities which did not produce any proton radiation on the earth. The selection of these flares was made according to the diagrams published in [8]\*. Information on these flares is cited in Table 3, and descriptions and sketches are provided for some of them.

The class III flares occur in complex multipolar groups of spots with strong fields. The flares with a point-3 intensity in the groups are followed by appreciable changes in the configuration of the poles, but these changes are not as great as in the case of the proton flares. We will examine several groups of spots where flares with point-3 intensity have occurred.

The flare of 1 May 1958 took place in a very long and complex group of spots 13,197 which appeared from behind the edge of the sun on 27 April. The flare originated in the head part of the group. Several weaker flares occurred in the same region. After the flare, the 22 S, 16 S and 15 N nuclei drew somewhat closer together. But the 17 S nucleus was found to have moved to the side. The large 22 S nucleus broke up into three separate nuclei -- 20, 22 and 20 S.

---

\* We are indebted to A. S. Dvoryashin for his advice in the selection of these flares.

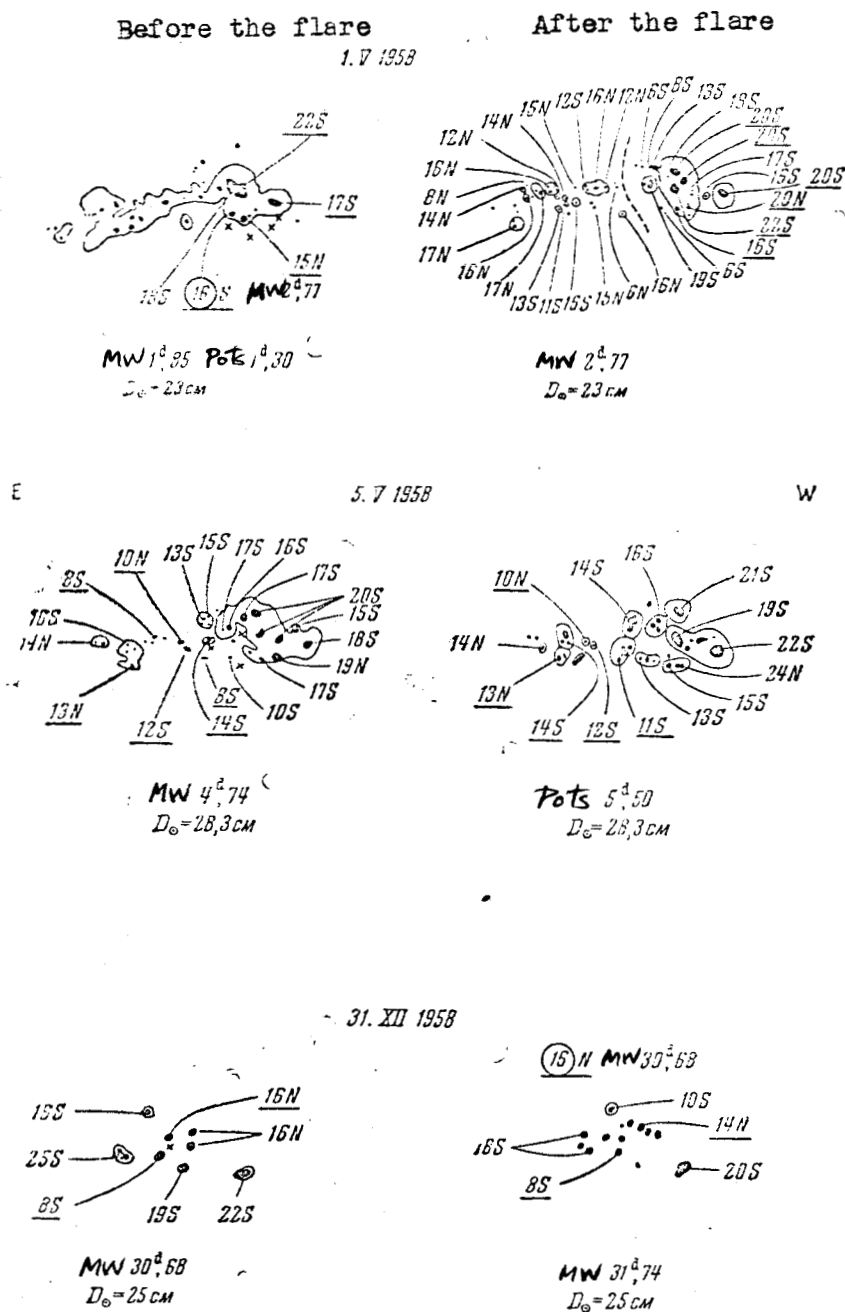


Fig. 3. The configuration of the spots and their magnetic fields involved in the class III flares

The flare of 5 May 1958 occurred in the same group as the flare of 1 May. By 5 May the spots in the head part of the group were clearly broken up. The flare occurred approximately in the central portion of the group. Almost all of the nearby poles drew closer together after the flare. Only the 14 S pole was found to have moved a considerable distance from the 12 S and 10 N poles.

Table 3

No.	Date	Intensity Points	Observation time		Coordinates
			beginning	end	
1	22.VII 1957	3	09 <sup>h</sup> 53 <sup>m</sup> E	11 <sup>h</sup> 50 <sup>m</sup> I	N 17 E 51
2	16.X	3	01 52	02 02	S 17 E 21
3	2.XII	2+	10 55	12 00	S 17 W 34
4	1.V 1958	3	21 15	22 42	S 18 E 15
5	5.V	3	03 56	04 47	S 18 W 20
6	19.VI	3	09 40	12 10	N 13 W 21
7	15.VII	3	22 36	23 14	N 12 E 3
8	29.VII	3	00 50	04 08	S 17 W 42
					S 17 W 44
9	31.XII	3	16 56	17 41	S 18 W 34

The flare of 31 December 1958 occurred in the group 13,803 which had appeared from behind the edge of the sun on 21 December. The group covered a large area and consisted of a considerable number of spots. The flare occurred in the central part of the group which revealed considerable structural changes after the flare. The group of nuclei 16 N was moved to a side and broken up, and the nuclei 8 S and 16 N, on the other hand, drew closer together.

IV. Flares with an Intensity of 2 and 2+ without Recorded Cosmic Radiation Effect

Class IV includes the flares with an intensity of 2 and 2+ which produced no geophysical effects (Table 4). Their selection was made in the same way as the class III flares. Descriptions and sketches of some of them are provided.

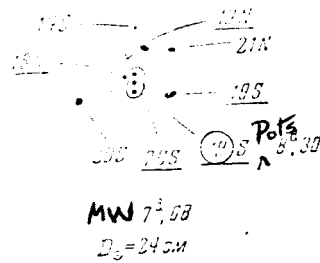
Table 4

No.	Date	Intensity Points	Observation time		Coordinates
			beginning	end	
1	4.VII 1957	2	11 <sup>h</sup> 34 <sup>m</sup> E	11 <sup>h</sup> 54 <sup>m</sup> E	N 12 E 39
2	7.IX	2	21 34	22 52	N 13 E 43
3	9.IX	2	07 55	08 55.1	N 12 E 22
4	30.IX	2	16 57	17 50	N 25 W 37
5	19.XII	2+	07 57	10 15	N 20 E 13
6	10.II 1958	2+	13 20E	14 11	S 13 W 64
7	27.III	2+	15 34	17 10	S 16 E 23
8	6.V	2+	06 35	07 10	S 16 W 37
9	19.V	2	10 52	12 05.1	S 17 W 50
10	1.VI	2	03 10E	04 19.1	S 17 E 12
11	4.VI	2	21 47E	23 56	N 17 W 58
12	11.VI	2+	20 37	21 20	N 41 W 12
13	14.VI	2	11 18	11 53	N 14 E 47
14	13.IX	2+	09 04	10 25	S 16 W 58

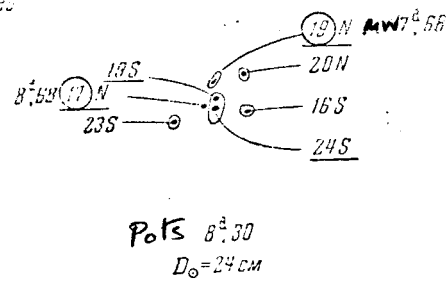
Just like the classes of flares discussed above, these flares originated in complex and large groups of spots. They were also followed by certain changes in the configuration of the nearby spots but these changes are considerably smaller than in the class I, II and III flares. Below is a description of several groups where flares with intensities of 2 and 2+ occurred.

Before the flare

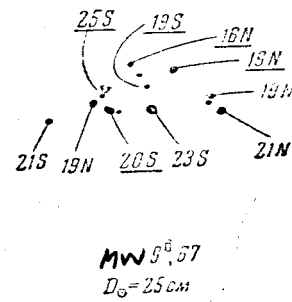
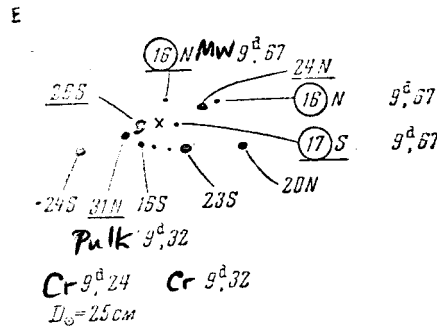
7 IX 1957



After the flare



9. IX 1957



27. III 1958

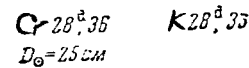
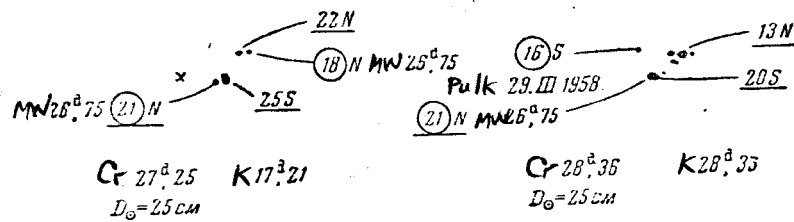


Fig. 4. The configurations of the spots and their magnetic fields involved in the class IV flares

The flare of 7 September 1957 occurred in the group 12,596 which had appeared from behind the edge on 4 September. That was a very long group consisting of a large number of large spots of various polarity. The flare originated near the central part of the group. After the flare, the 19 N pole drew appreciably closer to the 18 N and 19 S poles.

The flare of 9 September 1957 occurred in the same group as the flare of 7 September. It originated approximately in the center of the group. No changes were noted in the configuration of the spots after the flare (see sketch). The flare was observed from our observatory and described in detail in [10].

The flare of 27 March 1958 occurred in the small group 13,103 of fairly large spots which had appeared from behind the edge on 21 March. After the flare, the 21 N and 25 S nuclei were seen to merge into a single nucleus.

## 2. THE FLARE-PRODUCED CHANGES IN THE MAGNETIC FIELDS

### (Modelling Data)

The data listed in Part One on the magnetic fields of the groups of spots where flares had occurred were subjected to a close examination and a comparison was made of the intensities and arrangement of the spots before and after the flare. Inasmuch as the flare phenomenon is apparently based on the conversion of the magnetic field energy to thermal energy and plasma radiation energy [21], it is natural to look for a connection between the magnitude of the flare and the changes in the configuration and intensity of the magnetic field. Attention was first called to the changes ("destruction")

of the field in the neighborhood of the flares and, particularly, the changes of the field gradients in the zero points produced by the flares in [22], and to the changes in the configuration of the spots produced by the flares in [23 and 24]. From this point of view it may be expected that the most powerful proton flares will be accompanied by the greatest changes in the arrangement and intensities of the basic carriers of magnetic fields, the sun spots of the group in which the flare occurred.

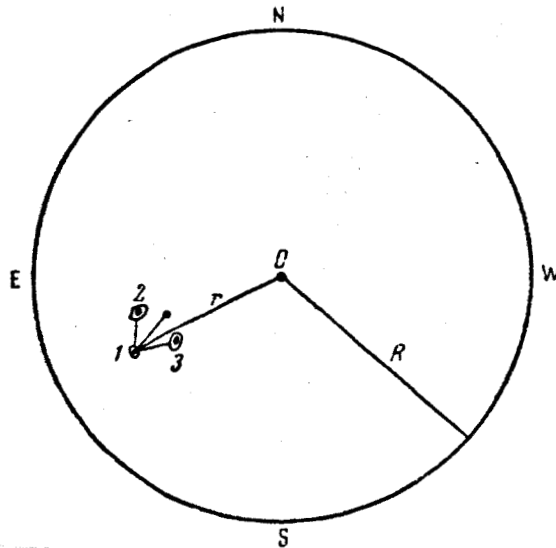


Fig. 5. Reduction of the arrangement of the group to the visible center of the disc

Digressing temporarily from the sizes (areas) of the spots, and considering the arrangement of their geometric centers and the intensities of their fields, we can compare the configuration produced by the point poles with a fixed intensity before the flare and after it. Such a comparison obviously requires a correction of the configuration for the effect of the

future contraction that will increase toward the edge of the disc. If  $r$  is the average distance from the center of the sun to the group of spots (1-3 in Fig. 5), and  $R$  the radius of the sun's representation, then the magnitude  $\frac{r}{R} = \sin \theta$ . Let  $a_1, a_2$ , etc. be the projections of the distances  $d_{12}, d_{13}$ , etc. between the spots in the direction of  $r$ , then these projections (released through the perspective contraction) reduced to the principal center, will be

$$x_1 = a_1 \sec \theta, x_2 = a_2 \sec \theta, \text{ etc.}$$

Actually (as long as  $\sec \theta \leq 1.5$ ) it is possible to ignore the changing radius-vector  $r$  within the group and take an average for the entire group (if it is not very scattered). If the group is closer to the edge of the disc, the position of each spot should be corrected separately. That is why in most cases one of the spots of the group is taken as the origin of coordinates 0, the direction of the radius-vector from the center of the solar disc to that spot is taken as the x-axis, the projections  $x_1, x_2$ , etc., are then measured off from point 0, and the distances of the spots 2, 3, etc. are transferred from direction  $r$  without changes. They apparently do not have to be corrected for the projection. By the position of the spot is meant the position of its geometrical center. This gives us the spot configuration corrected for the contraction and reduced to the visible center of the solar disc. All the configurations referred to hereafter are thus corrected for future contraction in the sense of the position of the spots; the areas of the spots have been corrected for contraction according to well known ratio  $S = S_0 \cdot \sec \theta$ , where  $S_0$  is the uncorrected area. Shown in Figs. 6 and 7 are similar configurations of groups of spot-poles nearest to the class I and III flares, respectively

(the flares are indicated by a cross, according to the data cited in paragraph 1) before the flare (above) and after the flare (below); the intensity of each pole is indicated (for its determination see Part 1). The diameter of the sun in Figs. 6 and 7 is always 250 cm, except for 15 November 1960 when  $D_{\odot} = 140$  cm.

The most difficult problem is the selection of the spots "responsible" for the configuration or structure of the magnetic field in the region of the flare. Two or three low intensity and small area spots which are close to each other and to the area of the flare can play a greater part in the formation of the magnetic structure than far away but larger spots, especially if such spots are considered as sources of a dipole field which changes a great deal with distance (see below). In a number of cases, such as the flares of 3 July 1957, 20 October 1957, 7 July 1958, 16 August 1958, 1 April 1960, 12 November 1960 and 15 November 1960 the situation was fairly simple and obvious; however, in the case of the flares of 22 August 1958, 28 September 1958 and certain others the situation was complicated by the fact that they originated in the groups including many small spots. In some cases the magnetograms and motion picture films made by us earlier facilitated this selection of spots (see Part 3).

The most conspicuous item in Fig. 6 is the extension of the configuration of the repulsion of the poles after the flare. This effect appears to be prominent in every case except on 1 April 1960 when the poles drew closer after the flare. The discrepancies in the results on the displacement of the spots during the flares in this work and in [23] is probably due to the following circumstance. Here the displacement of the spots is considered in relation

to the zero point, that is, in relation to the origin of the flare, whereas in [23] the displacement of the spots was considered in relation to the flare in a developed state (which possibly represents a surge of matter from the zero point and may be located far away from it).

This situation is explained in Table 5 which cites the relative changes of the distance between the poles  $\delta R/R$  of all the above discussed powerful class I proton flares.

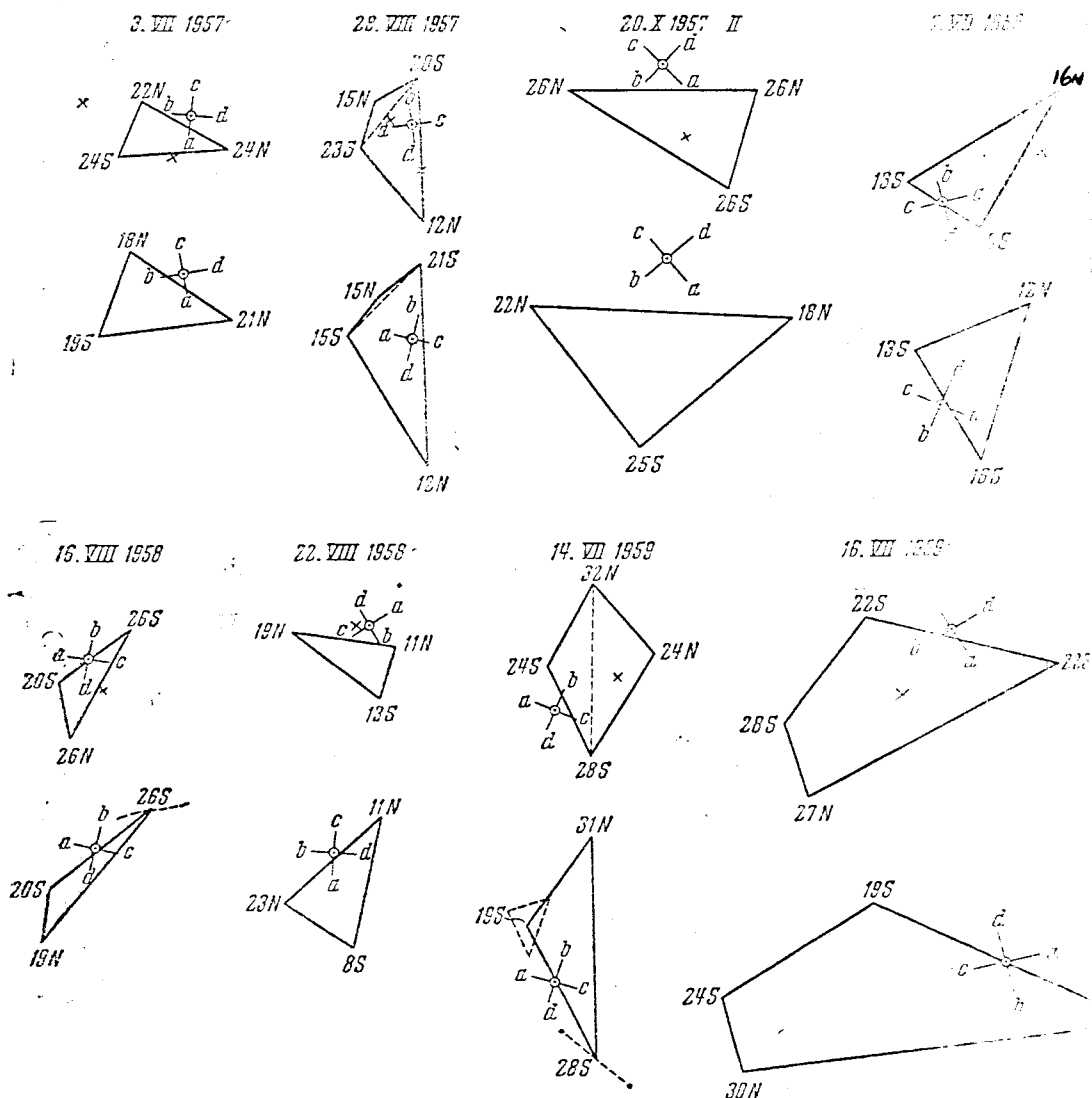


Fig. 6. The configuration of spots involved in class I flares

Top: before the flare;  
Bottom: after the flare.

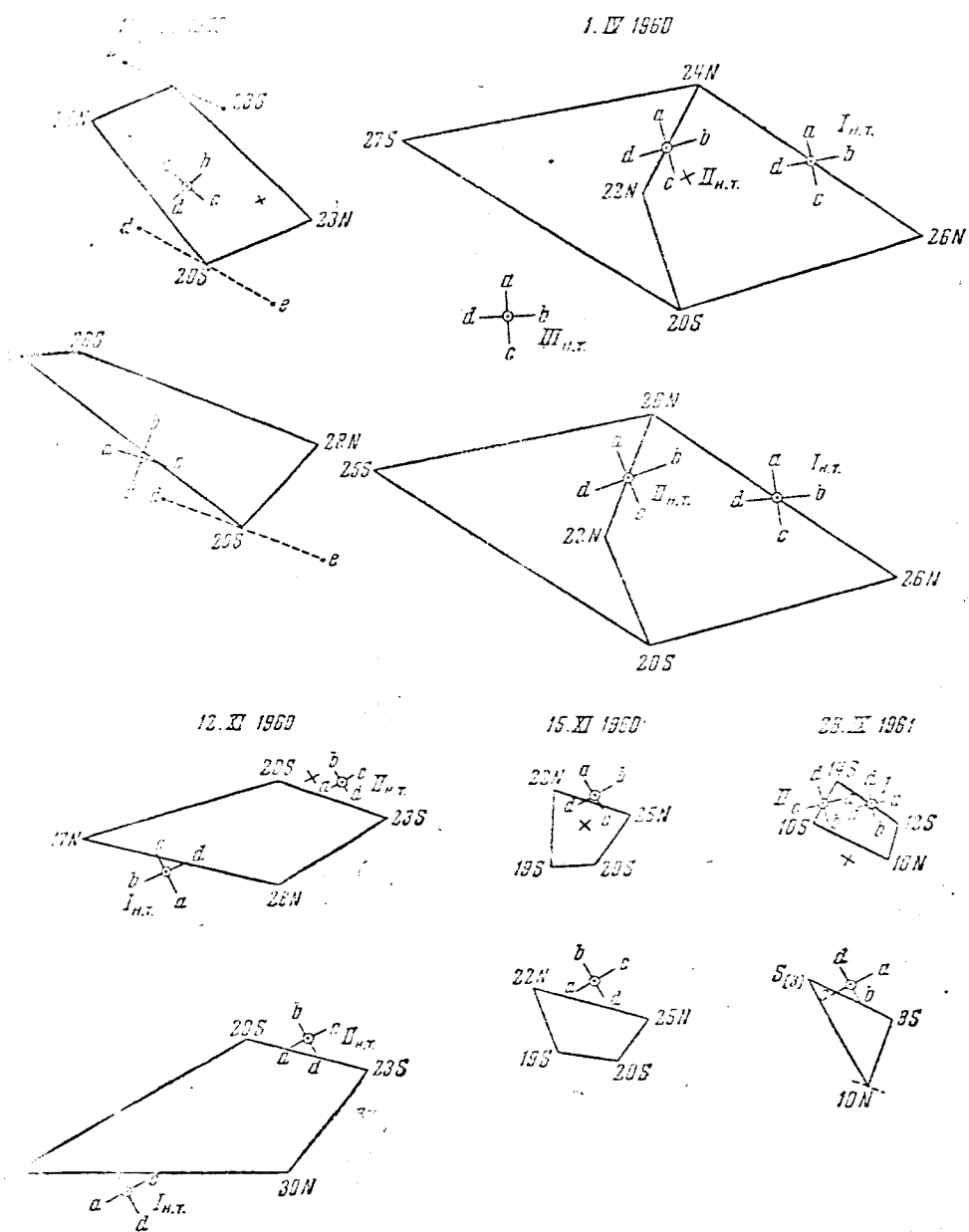


Fig. 6. Continued

The  $\delta R/R$  are listed in the first column for the opposite poles in which  $R$  is the smallest; the second column contains the same data, but  $R$  is the largest, and in the third column are the  $\delta R/R$  changes of the similar poles. For the opposite poles, in almost all the cases (except four)  $\frac{\delta R}{R_{\min}} \leq 0, \frac{\delta R}{R_{\max}} > 0$ , and for the similar poles  $\frac{\delta R}{R} > 0$  (except one case); the average values cited below clearly indicate that in the case of a three-pole configuration one of the two (farthest) similar poles is pushed out, and the pair of the nearest opposite poles draws somewhat closer together -- if a comparison is made of the configuration before and after the flare. This is schematically shown in Fig. 8: the pole  $S_1$  after the flare is pushed out into the position of  $S'_1$ , and the pole  $S_2$  gets closer to  $N_1$  and becomes point  $S'_2$ . A careful comparison of the poles' intensities before and after the flare (Fig. 6) shows that this process is due to the fact that one of the two similar poles with a decreasing intensity is pushed out (flares 2, 3, 4, 8, and 13 in Table 5), or that the intensity of its competitor is rising sharply. This is also due to the growing field of the pole of the opposite polarity  $N_1$ , which is close to the competitor (flares 6 and 9). On the average, the poles of different polarity do not draw closer to each other a great deal, although there are some cases when the polarities come in contact with one pole "absorbing" the other, as in the flare of 27 March 1958 for example. In three cases (flares Nos. 1, 7, 13) the simultaneous divergence of all the poles was accompanied by a diminishing intensity. Thus if we considered only the intensities of the poles we would get an extremely motley and unclear picture, but in combination with their changing position the re-

construction of the field configuration becomes quite clear. The gist of that reconstruction is that one of the similar poles (of a three-pole configuration) is pushed out or two such poles are pushed apart (in the case of a four-pole configuration).

Table 5

№	Date	$\delta R/R$			№	Date	$\delta R/R$		
		$(NS)_m$	$(NS)_M$	$(NN)$			$(NS)_m$	$(NS)_M$	$(NN)$
1	3.VII 1957	+0,29	+0,63	+0,22	10	1.IV 1960	-0,06	+0,025	+0,09
2	7.VII	-0,30	+0,02	+0,50		1.IV	+0,04	+0,012	0
3	28.VIII	-0,12	+0,06	+0,14	11	12.XI	-0,31	+0,02	-0,23
4	20.X	-0,03	+0,88	+0,40		12.XI	-0,26	+0,32	+0,05
5	16.VIII 1958	-0,06	+0,41	+0,50	12	15.XI	-0,11	-0,15	+0,44
6	22.VIII	-0,42	+1,44	+0,30		15.XI	0	+0,16	+0,43
7	14.VII 1959	+0,13	+0,48	+0,23	13	28.IX 1961	+0,30	+0,77	+0,20
8	16.VII	0	+0,43	+0,48	Average . . . .				
9	18.VIII	-0,37	+0,33	+0,25			-0,078	+0,38	+0,27
	18.VIII	-0,05	+0,57	+0,60					

Whether this reconstruction is brought about by the flare or vice versa, it is difficult to say, and for our purposes it is not very essential. But the fact that it is the "weakest" (in point of intensity and remoteness) of the two competing similar poles that is pushed out or moves in one direction is a phenomenon that can easily be explained from the point of view of the elementary interaction of magnetic masses, dipoles, that is that the poles behave quantitatively in the same way as would poles of solid magnets. This conclusion does not contradict the usual concept of a field of single spots as a field of a dipole or a solenoid top. The investigations made in [25], for example, showed that the law of the dipole field  $M\rho^3 = \text{const}$ , where  $M$  is the magnetic moment of the spot ( $M = HS$ ,  $H$  denotes intensity and  $S$  the "volume" of the spot) applies to the majority of the single spots. The concept of a fan

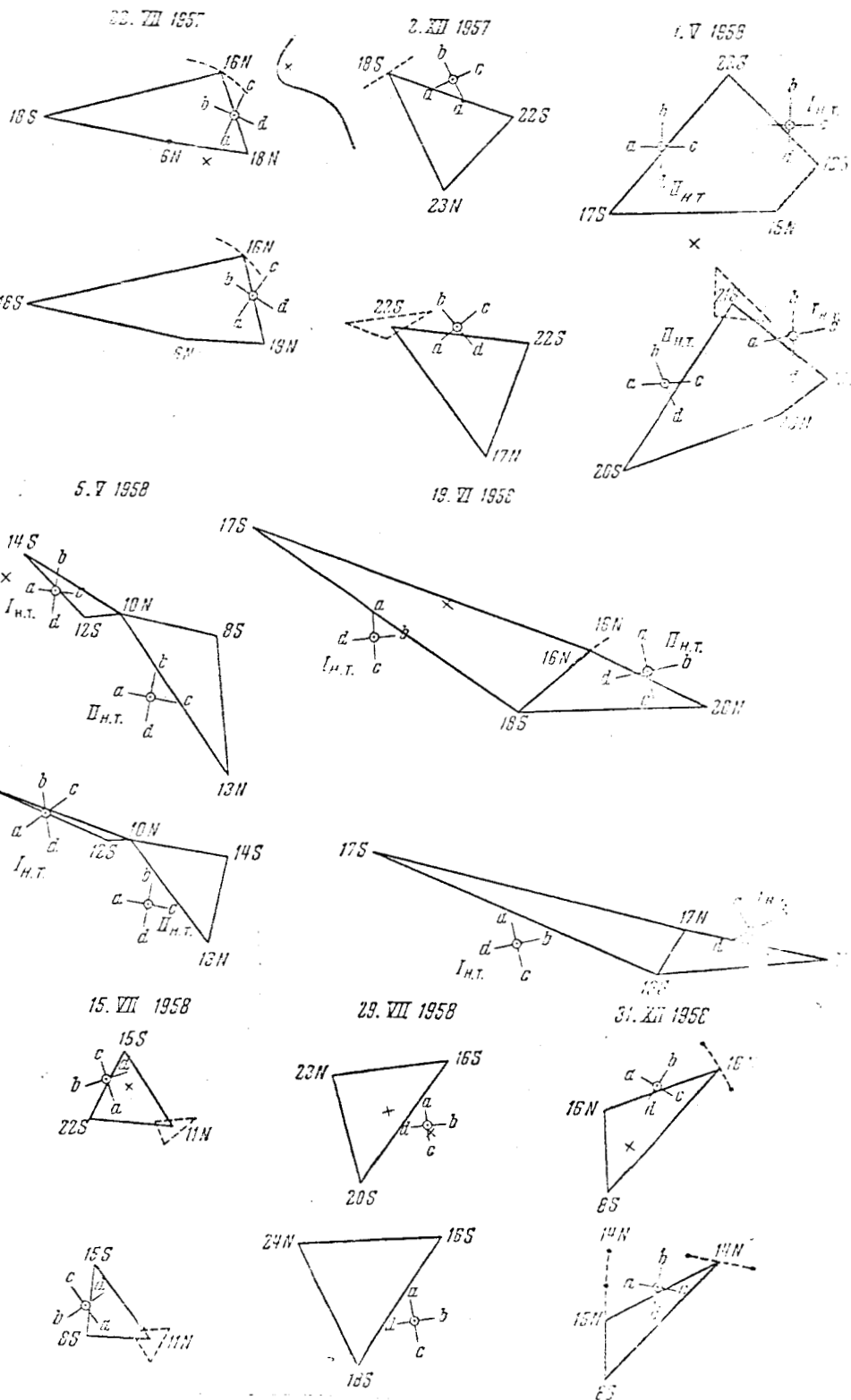


Fig. 7. The configuration of spots involved in class III flares

Top: before the flare;  
Bottom: after the flare.

of lines of force similar to the field of a solenoid top was first introduced in [26] and then developed and substantiated in [27]. Of course such a concept of the field of a spot is on the whole approximate, and it does not take into account the possible fine structure of the field or the occasional appearance of two different polarities or transverse fields within a single penumbra or even nucleus as indicated in the investigations of [28] and [29], for example. But whatever that structure, at a fairly large distance from the spot nucleus its field may in the first approximation be considered as the field of a solenoid top or dipole. The entire further analysis of the field configurations is based on such a concept.

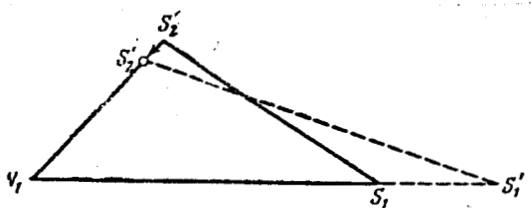


Fig. 8. A characteristic change of the configurations produced by flares

If we are interested in the detailed structure of the field, for example, if we want to know whether there are zero points and lines of field and where they are located, what is the gradient of the field near the zero point, the location of the regions of the largest and smallest transverse or longitudinal components of the field, etc., we can find the reply to these questions only by solving the problem of the interaction of  $n$  dipoles with prescribed moments located at preset distances. Even in the very simple case

of three poles with similar moments located at the angles of an equilateral triangle, the problem involves considerable calculation difficulties. The question naturally arises whether it is possible to model solar magnetic fields.



Fig. 9. Installation of modelling magnetic fields of spot groups

It is obviously possible to think of laboratory modelling as a method designed to facilitate calculations if we become convinced that similarity ratios facilitating a change from a laboratory to a solar model when the scale changes  $10^7 - 10^8$  times can be applied to the field characteristics in which we are interested. We will select a neutral point of the field -- its existence, location and field gradient in its neighborhood -- as such a basic characteristic. The reason for this is not only that the flares apparently originate in the neutral points when large field gradients

are available near them [21, 22] but also because it is easy to find a similarity ratio for the neutral point.

A small installation (Fig. 9) designed to shift and arbitrarily introduce three solenoids along two coordinates was developed for the purpose of modelling the fields of solar groups in a laboratory. The solenoids can produce a field from 0 to  $10^3$  gauss with a current up to 2.5 amps and 220 volts dc. The removable rods of different thickness used in them made it possible to model various spot areas (dipole areas; the umbra areas were considered). The ratio between the pole diameter (average) and the dipole length (of the magnet and solenoid) amounted on the average to  $\sim \frac{1}{10}$ , including the screen thickness. This ratio was selected from considerations of similarity (see below), in the belief that the depth of the power tube, the average spot, is probably  $\sim 10$  times greater ( $\sim 10^4$  km) than the average size of the spot ( $10^3$  km) [30].

We will examine a three-pole configuration  $NS_1S_2$  for the purpose of establishing the similarity ratio, and begin by changing only the intensity of the poles and leaving the intensity relations and distances between the poles unchanged (the initial configuration is shown in Fig. 10). It is then easy to see (as we have done experimentally) that the position of the neutral point  $m$  does not change and the intensity of the field at a prescribed distance from the neutral point changes in proportion to the field intensity of the poles. In other words, the relation of the field gradients near the neutral point to the dipole moment of any of the poles does not change with the changing moments of the poles if only the relation between the moments remains

unchanged. That means that in the modelling it is necessary to observe the same relation of the moments as on the sun. We will now change the distance between the poles, preserving the similarity and not changing their moments. It is thus easy to see that the position of the neutral points is preserved just as in the initial configuration; its distance from the poles and the straight lines connecting them changes in a similar way. The question arises as to how the intensity of the pole at a present distance from the neutral point (in units distance between the poles) changes in this case.

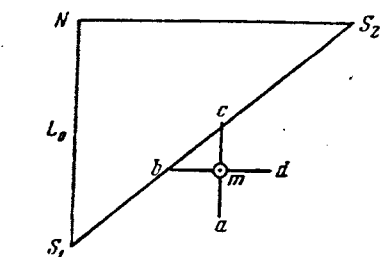


Fig. 10. The configurations used in the study of similarity ratios  $H(S_1)=1.2 H(N)$ ;  $H(S_2) = 1.5 H(N)$

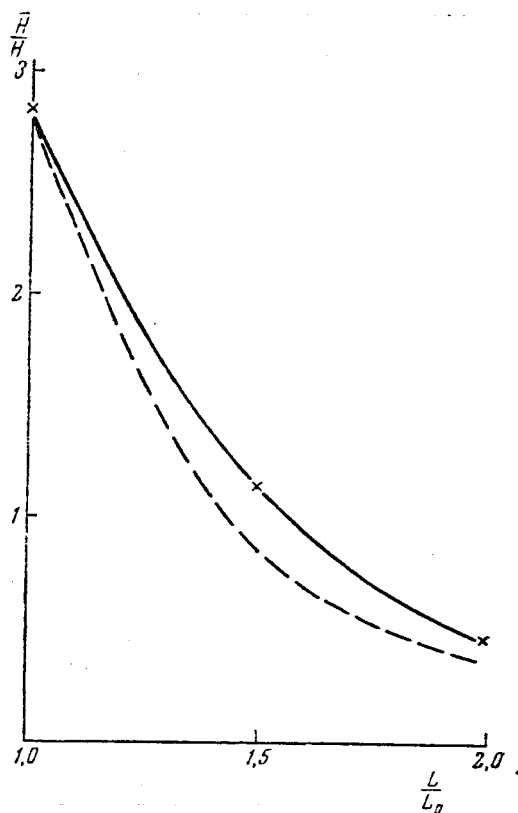


Fig. 11. The changing intensity near the zero point produced by the changing scale of the configuration and the unchanged dipole moments

Solid line -- observation, dashed line --  $(L/L_0)^{-3}$

Fig. 11 shows that this intensity for the configuration we have selected diminishes somewhat slower than according to the law  $(L_0/L)^3$ , where  $L/L_0$  is the linear scale of the configuration (in units of the initial  $L_0$ ). Further, it can easily be seen that, in accordance with the well known theoretical conclusions, the intensity in the neighborhood of the zero point under consideration saddlepoint surface) always changes (regardless of the scale) in proportion to the distance of  $x$  from the zero point: the larger the scale of configuration the greater the linearity region. The laboratory modelling which we have done on the scales  $\frac{L}{L_0} = 1.0; 1.25; 1.50; 1.75; \text{ and } 2.0$  shows that there is a region of guaranteed linearity  $H$  near a zero point, say  $a/a_0$ ; it is determined approximately by condition  $\frac{a}{L} \leq \frac{1}{10}$  beginning with  $L_0 \geq 5 \text{ cm}$ , if the field intensity at the poles does not exceed  $10^3$  gauss.\* Thus in this region near the zero point the field gradient changes as  $H/a$ . The index in the law of changing  $(L_0/L)^n$  in this case depends to some extent on the type of the configuration, and in the cases under consideration we obtained  $n$  in the range between 2.4 and 3, which also depends on which direction from  $m$  ( $a, b, c, d$ ) the field is measured.

For purposes of simplification, we will assume that  $n = 3$ , that is, that the field intensity near the neutral point (in the region of field linearity) changes as  $(L_0/L)^3$  with the changing scale of the configuration and the invariable magnitude of the dipole moment. However, if we change from the solar to the laboratory model and vice versa we have no right to

---

\* The measurements in Fig. 11 apply to point  $a/a_0$ .

leave the dipole moment invariable because it changes as the polar volume, that is, as  $(L)^3$ . As the field intensity near the neutral point changes in proportion to the dipole moment, the field gradient near the neutral point should change as  $\left(\frac{L_0}{L}\right)^3 \left(\frac{L}{L_0}\right)^3 \frac{L_0}{L} \sim \frac{1}{L}$ , if the relation between the dipole dimensions and the characteristic scale remains the same for the laboratory model and the Sun. The validity of this can easily be proved also by the simplest example of interaction between the two poles  $N_1$  and  $N_2$  of the dipoles, located along the  $N_1 N_2$  straight line with the distance  $R$  between them. Let  $x_0$  be the distance of the neutral point from the  $N_1$  pole. The field intensity at distance  $x$  from  $N_1$  will be

$$H = \frac{m_1}{x^2} - \frac{m_2}{(R-x)^2}, \quad (1)$$

where  $m_1, m_2$  are the moments of poles  $N_1$  and  $N_2$ . In the neutral point we obviously have  $(R-x_0)^2 m_1 = m_2 x_0^2$ , whence

$$\frac{R-x_0}{x_0} = \sqrt{\frac{m_2}{m_1}} \equiv \mu \quad \text{and} \quad x_0 = \frac{R}{1+\mu}. \quad (2)$$

We will further introduce the coordinate  $x' = x - x_0$  which is the distance from the neutral point; then (1) will be

$$\frac{H}{m_1} = \frac{1}{(x_0 + x')^2} - \frac{1}{\left(x_0 - \frac{x'}{\mu}\right)^2},$$

expanding this into a series by  $x'/x_0$  degrees and limiting ourselves to linear terms, we will get

$$\frac{x_0^2}{m_1} H = 1 - 2 \frac{x'}{x_0} + \dots - \left( 1 + 2 \frac{x'}{\mu x_0} - \dots \right) \cong -2 \frac{x'}{x_0} \frac{1 + \mu}{\mu}$$

or

$$H = - \frac{2m_1}{x_0^3} \frac{1 + \mu}{\mu} x'. \quad (3)$$

Thus the field in the small region of the zero point  $\left( \frac{x'}{x_0} < 1 \right)$  is proportional to the distance from the zero point. Further, as  $m_1 \propto L^2$ , and  $x_0 \sim L$ , where  $L$  is the characteristic scale of the configurations, then  $\nabla H \sim \frac{1}{L}$ , if the intensity relation of poles is unchanged. A similar reasoning can easily be applied to the interaction between two dipoles; in this case  $H \sim \frac{m}{x_0^4} x' \sim \frac{L^2 h}{L^4} x' \sim \frac{x'}{L}$ , if  $h$  length of the dipole is proportional to  $L$ . In the case of a triple pole with a zero point lying on a  $N_1 N_2$  straight line, the reasoning will be quite similar in the calculation of the intensity along the  $N_1 N_2$  axis. This important characteristic of the field gradient near the zero point  $\nabla H \sim \frac{1}{L}$  facilitates the successful modelling of the situation at the zero point, by knowing the absolute intensity of the spots producing that situation, and without resorting to the lengthy and cumbersome calculations. This is in itself an important argument in favor of selecting a zero point as a characteristic place of a field whose behaviour will in time reflect such characteristics of the group development as the magnetic moments of spots, their mutual arrangement and distances within the group.

All these considerations enabled us to use the above-described laboratory

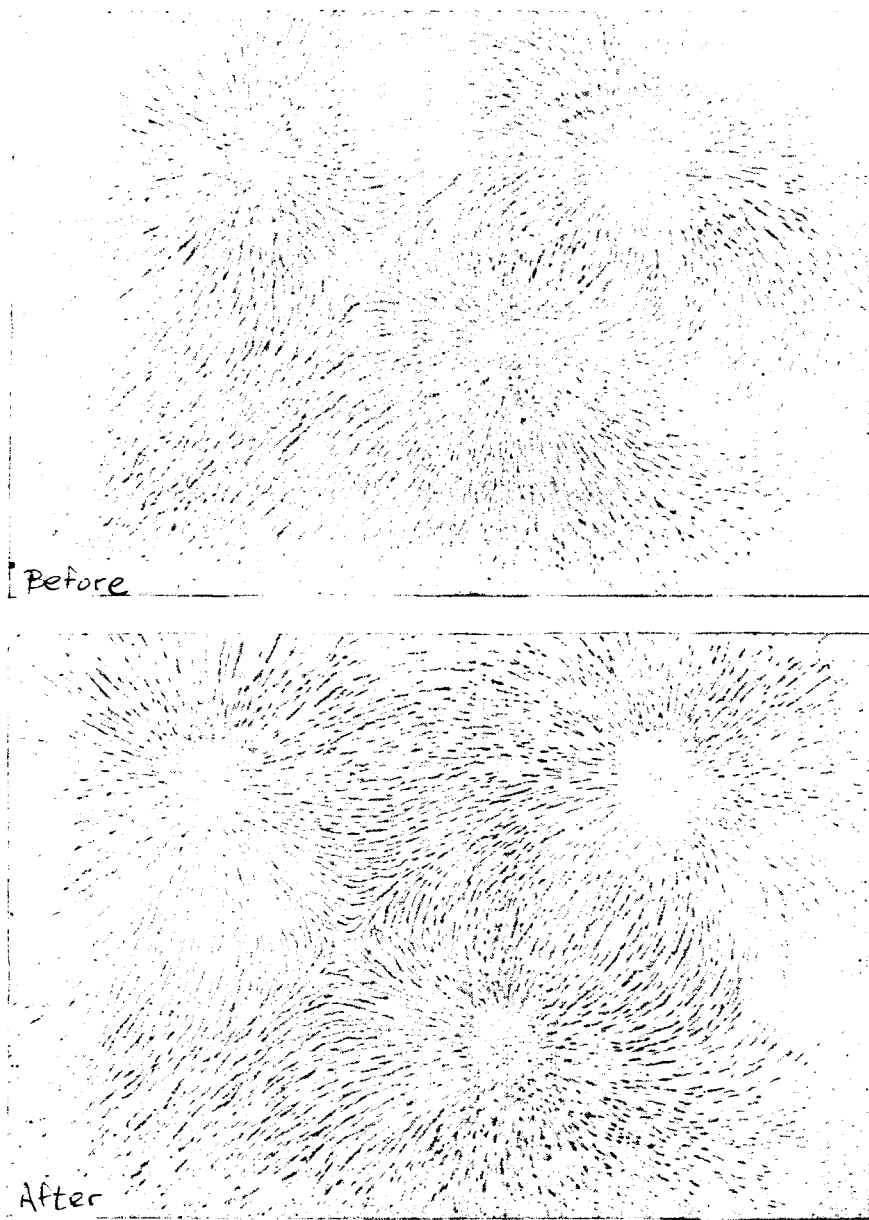


Fig. 12. Examples of magnetic lines of force involved in the modelling of spot configurations before and after the flare

(see also pp. 47 and 48 of the text)

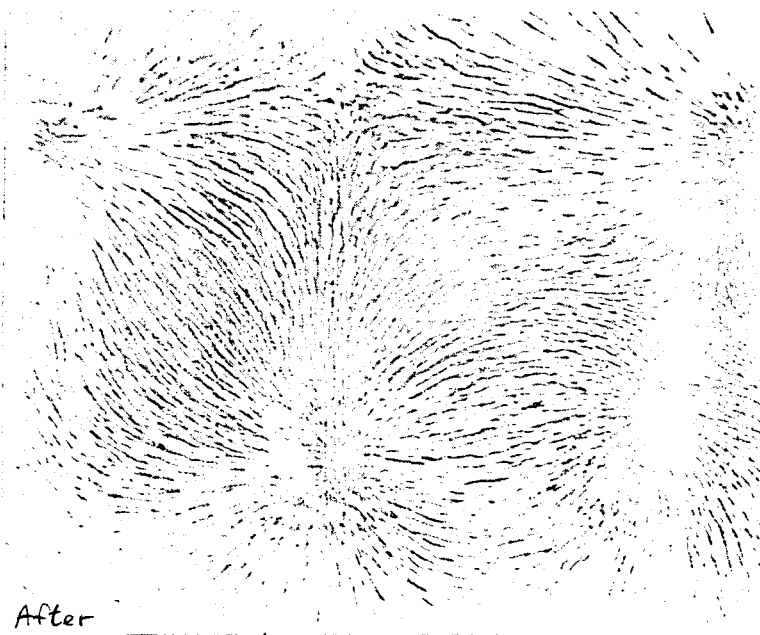


Fig. 12. Continuation

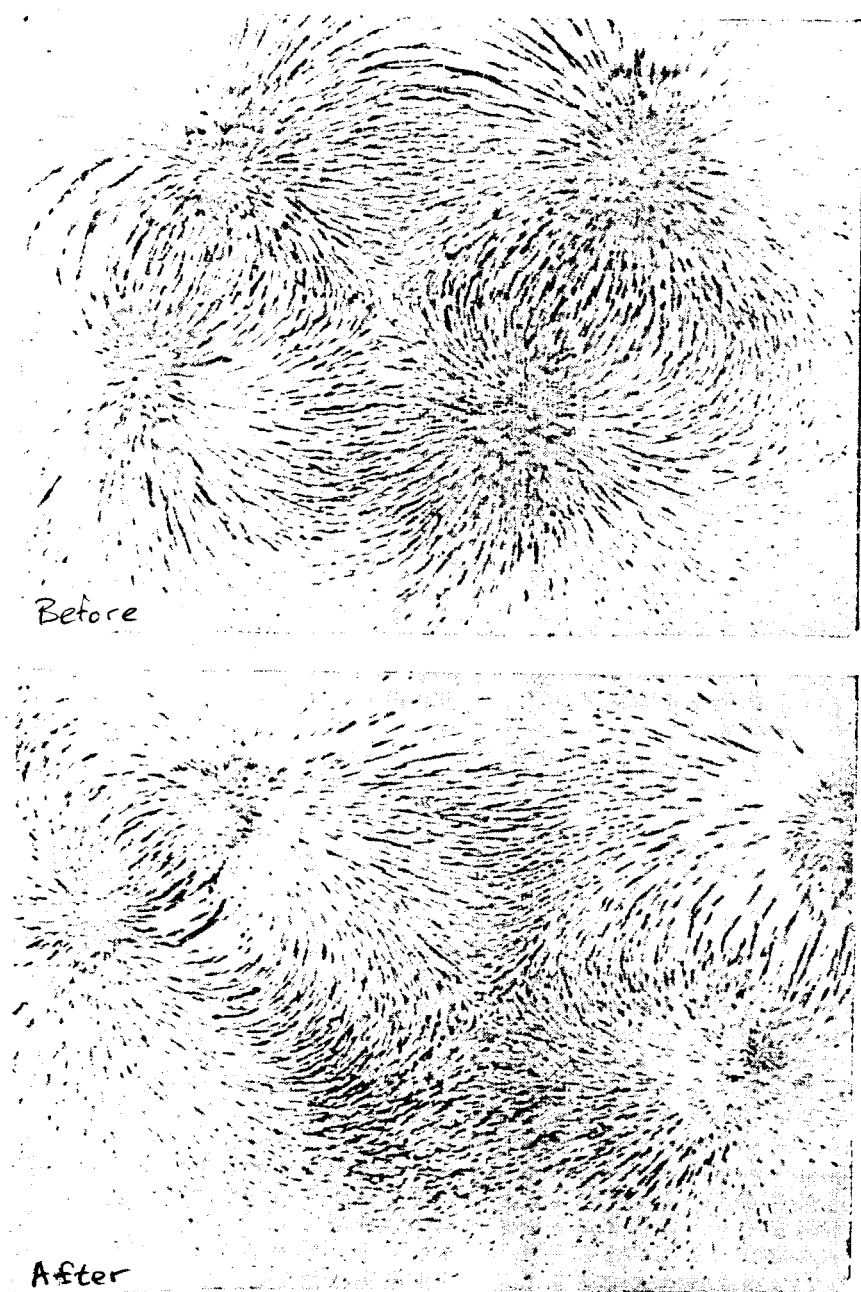


Fig. 12. End



Another essential modelling characteristic is that it is still either impossible to obtain direct observation data on the transverse fields in the groups of spots (at a fairly long distance from the spots of the magnetograph noise is  $\sim 100$  gauss, see [31]), or requires a very long processing time. But the type of modelling that enables us to get an approximate ideal of the transverse and longitudinal fields on the basis of the absolute field intensities in the spots, makes it possible to analyze and process a large volume of information based on the observation of the spot magnetic fields accumulated during the IGY at various observatories. We will examine group 29 which was observed by our observatory on 6 September 1961 as a concrete modelling example; this is the only case so far for which complete maps of the transverse field have been constructed in [29]. A comparison with a laboratory model in this case is of particularly importance and interest. A complete modelling of the field of this group would have required a fairly complex installation consisting of 7-8 magnets which we did not have; we therefore had to limit ourselves to the western part of this group, leader A, its satellite B, intermediate spot C and the westernmost part of the tail spot D which is close to the leader (see description of this group in [29]). A sketch of this group with a polaroid grid determined by the use of a  $\frac{1}{4}\lambda$  plate and a line shifter determined by the magnetic fields is shown in Fig. 13, and Fig. 14 shows the diagram of the selected configuration (corrected for the contraction of  $\sec \theta = 1.15$ ) with the solar diameter equalling 250 cm. Here the points denote the geometrical centers of the spot umbras for which these determinations were made; indicated in parentheses in the same place are the areas of the spot

nuclei (in square millimeters of the original sketch in the guide,  $1 \text{ mm} = 2''{,}5$ ). The sum total of this we will replace with four interaction centers A, B, C, D by selecting the position of the center in accordance with the position of the centers of the nuclei and their magnetic moments. The areas of these centers we will assume to be equal to the total areas of the individual nuclei (in parentheses), and the intensities as the average weights (weight is the area of the nucleus). In the group of C nuclei we will disregard the pole 17 N, and in the D group the pole 25 N, which may visibly distort our comparison.

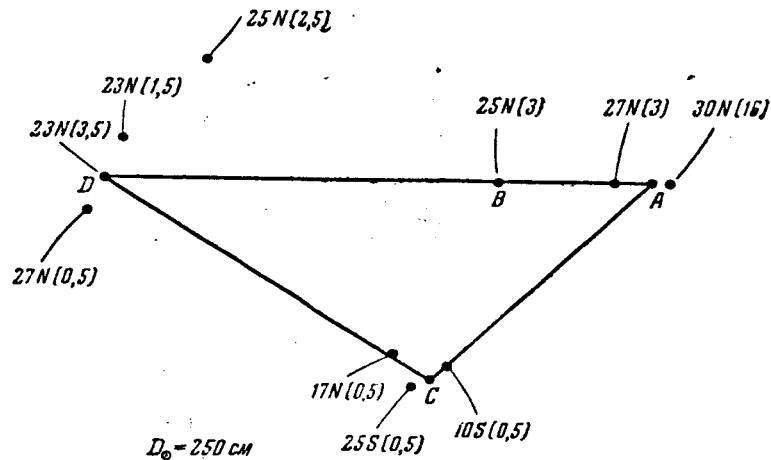


Fig. 14. The field configuration diagram of group 29  
(6 September 1961)

Table 6

Center	S	S'	$\bar{S}$	$\bar{S} \sec \theta$	d, mm	$d_0$ , mm	$d_p$ , mm	$d_0/d_p$
A	19	15	17	19,5	4,4	15,8	20	0,79
B	3	1,9	2,5	2,8	1,7	6,0	10	0,60
C	1	1	1,0	1,15	1,1	3,8	5	0,76
D	5,5	2,9	4,2	4,8	2,2	7,8	10	0,78

Average . . . . . 0,71

The finally adopted modelling diagram is shown in Table 6. Here  $S$  is the area indicated in the sketch,  $S'$  the area shown in the photoheliogram,  $\bar{S}$  the finally adopted average of both areas,  $\bar{S} \sec \theta$  is the area adjusted for the projection, and  $d$  the diameter of an equivalent spot.

$$d = \sqrt{S \sec \theta}.$$

It has normally been convenient to model with the Sun's diameter equalling 250 cm; the sizes of the spots reduced to that scale are indicated by  $d_0$  (in the case of observations through a tower solar telescope,  $d_0 = 3.57 d$ ). We have had at our disposal rods with diameters of  $d_p = 5, 10, 15, 20$  mm. Therefore, if we use these pole sizes for modelling purposes (see the adopted  $d_p$  in column 8, Table 6), then all the magnitudes proportional to the magnetic moment of the spots (for example, the field gradient at the zero point) should be corrected by multiplying them by ratio  $(d_0/d_p)^2$ . In our case, this ratio equals  $(0.71)^2 \sim 0.50$ . However, if we are not satisfied with the resulting scale ( $D_\odot = 250$  cm), and we have to increase it (say,  $n$  times), it becomes obvious that in order to preserve a constant relationship between the spot sizes and their mutual distance (the same as on the Sun), we must multiply the magnitudes which are proportional to the spot moments by  $n^2$ , if the modelling does not change the pole sizes (or the latter would have to be increased  $n$  times).

After the modelling program has been set up, it is more convenient to model the lines of force of the transverse field in the "photosphere" plane in the form of a photograph of iron shavings spread evenly on a screen supported by the ends of the poles. A photograph of the group 29 model (6 September 1961) is shown in Fig. 15. The dashed lines indicate the directions

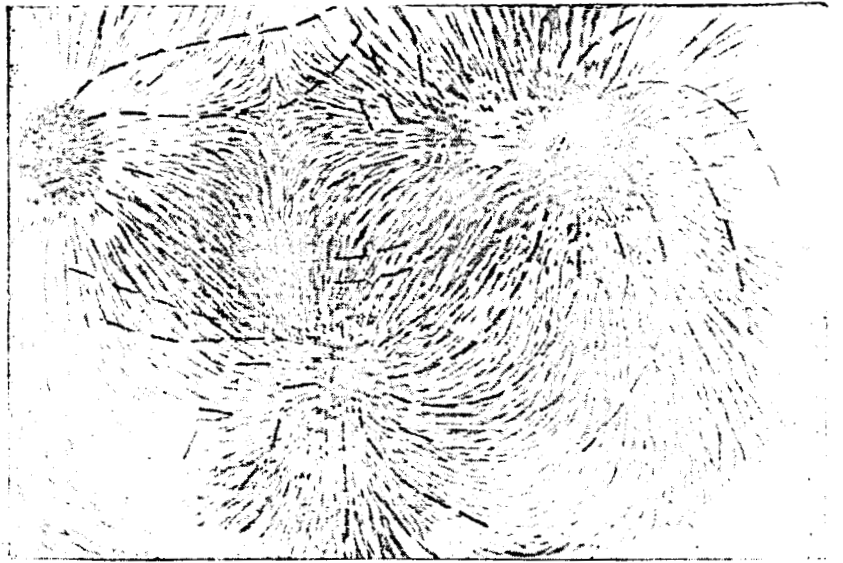


Fig. 15. A comparison of the model and the actual lines of force (dotted lines) in group 29 (6 September 1961)

of the lines of force actually measured in [29]. Digressing from the vortex field structure of spot A, we see that the actual zero point has been shifted to the right toward spots A and B as compared to the model point, which may be due to the fact that we have neglected the fairly important pole 25 N located between D. and B. But it should be borne in mind that the definition of the transverse fields in the zero point region is not very certain (error: ~100 gauss), and the localization of that point is therefore inaccurate. The deviation of the model from the actual picture above pole C is due to our neglect of polarity 17 N which prevents the lines of force running from D to A to join above pole C (compare diagram on Fig. 14). Finally, some of the lines of force running from C to D do not join on D but on a stronger pole which follows immediately after D and which has not been taken into account at all. It should also be borne in mind that the actual picture has not been

adjusted for the projection effect. Despite all these differences, connected with the imperfection of the model, the general nature of the field can be modelled correctly if we do not count the vortex structure near spot A which on general principles cannot be modelled by the dipole field without taking account of the plasma surrounding the spot.

Similar methods were used to model the fields before and after the flare in the case of all the above discussed 47 flares for which it was possible to find reliable data on the magnetic fields since the beginning of the IGY (a description of the information is found in Part 1 above). The positions of the zero points, according to the model, are indicated on the actual field configuration by a point in a circle; indicated there also are the directions perpendicular to the lines of force (hyperbolas) along which the field gradient of the zero point was measured (Figs. 6 and 7). A comparison of the position of the zero points with that of the flares indicated by crosses is of no particular interest, as the universal data on the position of the flares are quite indefinite: in a number of cases they refer to the beginning of the flare in which case a comparison is impractical, and in a number of cases they refer to the phase of the following development of the flare which usually has no relation to the zero point. The coordinates of the flares in the Dodson catalog and Q. B. cannot be used to determine to which phase of the flare development they belong; from Figs. 6 and 7 we can see, for example, that in individual cases coincidences are true although some of the deviations amount to 2 - 3 heliographic degrees (which, it is true, is comparable to the difference in the determination of the flare coordinates

by different observatories).

The difference in the field gradients near the zero point measured by a flux meter of the model (in the area of field linearity) in various directions (indicated by a, b, c, and d in Figs. 6 and 8) is usually less than 30%, and we therefore indicate the average gradient in all directions. Indicated in Tables 7 - 10 are the modelling results for the above mentioned four groups of flares: proton flares with their effects observable by radiosonde (Table 7); flares which did not produce an effect on the radiosonde but a powerful absorption in the polar cap (PCA) (Table 8); flares of point 3 intensity which did not produce any effect at all (Table 9), and flares of points 2 and 2+ (Table 10).

Table 7

No	Date	$t_1$	$t_{\text{flare}}$	$t_2$	$\nabla H_1$ gauss/ km	$\nabla H_2$ gauss/ km	$\nabla H_a$ gauss	$\frac{\nabla H_a}{t_2-t_1}$ gauss/day	$\tau_{\text{flare}}$ day
1	3.VII 1957	3 <sup>d</sup> ,19	3 <sup>d</sup> ,30—3 <sup>d</sup> ,49	3 <sup>d</sup> ,56	0,56	0,23	330	890	0,19
2	28.VIII	28,30	28,34—28,58	28,81	0,44	0,09	350	700	0,24
3	20.X	19,73	20,69—20,75	21,33	0,28	0,085	195	122	>0,06
4	7.VII 1958	5,79	7,02—7,18	7,75	0,96	0,17	790	400	0,16
5	16. VIII	15,28	16,19—16,35	16,40	1,86	0,49	137	140	0,16
6	22.VIII	21,77	22,59—22,72	22,74	0,18	0,09	90	93	>0,13
7	10.VII 1959	9,30	10,09—10,38	10,67	—	—	—	—	—
8	14.VII	13,16	14,14—14,47	15,15	1,19	0,52	670	330	0,33
9	16.VII	16,33	16,89—17,02	17,65	0,18	0,078	100	78	0,13
10	1.IV 1960	1,35	1,36—1,56	2,18	0,62	0,73	-110	-125	0,20
11	12.XI	12,29	12,55—12,81	13,23	0,40	0,15	250	266	0,26
12	15.XI	14,32	15,09—15,18	15,25	2,48	0,60	1880	2000	0,09
13	28.IX 1961	28,25	28,93—29,06	29,24	0,17	<10 <sup>-2</sup>	170	162	0,13

Total 13 cases | Average . . | 0,78 | 0,27 | 404 | 410 | >0,182

The number of the flare is indicated in Tables 7-10 (each individual flare has its own number which is occasionally divided into a and b for different configurations); also the date of the flare; the time of the field measurements before the flare  $t_1$  and after  $t_2$ ; the beginning and end of the flare ( $t_{\text{flare}}$ ) and the average field gradient (in gauss/km) near the zero point before the flare  $\nabla H_1$  and after it  $\nabla H_2$ . These gradients enable us to estimate field intensity at a **certain** preset "standard" distance from the zero point. Such a distance is taken to be  $a = 10^3$  km.  $\nabla H_a$  (gauss) denotes the change of the field at that standard distance from the zero point, and  $\nabla H_a / t_2 - t_1$  gives us the average speed of the change of the field with time near the zero point (in gauss per 24 hours). Finally, the last column indicates the duration of the flare which also characterizes the power of the flare.

Table 8

No	Date	$t_1$	$t_{\text{flare}}$	$t_2$	$\nabla H_1$ , gauss/ km	$\nabla H_2$ , gauss/ km	$\nabla H_a$ , gauss	$\frac{t_2 - t_1}{24}$ , days	$t_{\text{flare}}$ day	
1	31.VIII 1957	30 <sup>d</sup> ,69	31 <sup>d</sup> ,54—31 <sup>d</sup> ,62	31 <sup>d</sup> ,71	0,28	0,45	-165	-162	>0,08	
2a	3.IX	2,69	3,59—3,71	3,67	0,58	0,47	110	113	0,12	
26	3.IX	2,69	3,59—3,71	3,67	0,80	0,19	610	620	0,12	
3	10.IX	9,67	10,10—10,13	10,40	0,76	0,23	530	725	>0,13	
4	11.IX	10,56	11,10—11,31	11,73	0,21	0,16	50	430	>0,21	
5a	21.IX	21,34	21,56—21,63	21,72	1,20	0,98	220	580	0,07	
5b	21.IX	21,34	21,56—21,63	21,72	0,13	0,11	20	53	0,07	
6	20.VIII 1958	19,73	20,03—20,06	20,23	0,50	0,16	340	68	>0,03	
7	26.VIII	24,69	26,00—26,06	26,24	0,30	0,15	145	93	0,03	
8	18.VIII 1959	18,18	18,43—18,53	19,17	0,16	0,017	140	142	0,10	
9	29.III 1960	29,23	29,28—29,37	30,26	0,08	0,028	152	147	0,02	
Total 11 cases					Average ...	0,45	0,27	225	284	>0,03

Table 9

No.	Date	$t_1$	$t_{\text{flare}}$	$t_2$	$\nabla H_1$ gauss/ km	$\nabla H_2$ gauss/ km	$\nabla H_a$ gauss	$\frac{\nabla H_a}{t_2-t_1}$ gs/day	$\tau_{\text{flare}}$ day
1	22.VII 1957	22 <sup>d</sup> , 22	22 <sup>d</sup> , 41—22 <sup>d</sup> , 54	22 <sup>d</sup> , 56	0,23	0,31	—80	—230	0,13
2a	16.X	15,46	16,08—16,09	16,49	1,19	—	—	—	—
2b	16.X	15,46	16,08—16,09	16,49	0,49	—	—	—	—
3	2.XII	2,23	2,45—2,50	2,70	0,23	0,26	—30	62	>0,02
4a	1.V 1958	1,30	1,88—1,94	2,34	0,30	0,18	120	115	0,06
4b	1.V	1,30	1,88—1,94	2,34	0,10	0,039	61	59	0,06
5a	5.V	4,74	5,15—5,21	5,50	0,17	0,032	94	123	0,06
5b	5.V	4,74	5,15—5,21	5,50	0,058	0,023	35	46	0,06
6	19.VI	18,71	19,40—19,50	19,71	0,11	0,08	31	31	0,10
7	15.VII	15,80	15,94—15,97	16,80	0,26	0,20	65	65	0,03
8	29.VII	28,21	29,04—29,17	29,23	0,12	0,064	52	43	0,13
9	31.XII	30,68	31,71—31,74	31,74	0,20	0,14	60	57	0,03

Total 12 cases | Average . . . | 0,18 | 0,13 | 63 | 83 | 0,07

Table 10

No.	Date	$t_1$	$t_{\text{flare}}$	$t_2$	$\nabla H_1$ gs/km	$\nabla H_2$ gs/km	$\Delta H_a$ gauss	$\frac{\nabla H_a}{t_2-t_1}$ gauss/day	$\tau_{\text{flare}}$ day
1	4.VII 1957	3 <sup>d</sup> , 56	4 <sup>d</sup> , 48—4 <sup>d</sup> , 50	4 <sup>d</sup> , 56	0,027	0,062	—35	—33	0,02
2	7.IX	7,68	7,90—7,95	8,30	0,040	0,036	4	65	0,05
3a	9.IX	9,32	9,33—9,37	9,67	0,081	0,051	30	67	0,04
3b	9.IX	9,32	9,33—9,37	9,67	0,075	0,024	51	110	0,04
4	30.IX	29,70	30,71—30,74	30,92	0,049	0,043	6	4,9	0,03
5	19.XII	18,70	19,33—19,43	19,68	0,100	0,087	23	23	0,10
6	10.II 1958	9,74	10,56—10,59	10,96	0,020	limb	20	26	0,03
7	27.III	27,25	27,65—27,72	28,36	0,017	<0,001	16	14	0,07
8	6.V	5,50	6,15—6,17	6,28	0,058	0,007	—11	—14	0,02
9	19.V	19,30	19,45—19,50	19,71	0,043	0,011	32	78	0,05
10	1.VI	31,60	1,13—1,18	1,32	0,068	—	68	94	0,05
11	4.V	4,78	4,91—5,00	5,84	0,040	0,010	30	30	0,09
12	11.VI	11,51	11,86—11,88	12,16	0,054	0,020	34	52	0,02
13	14.VI	14,32	14,47—14,50	14,73	0,077	0,087	—10	—24	0,03
14	13.IX	13,33	13,38—13,44	13,72	0,061	0,047	14	36	0,06

Total 15 cases | Average . . . | 0,054 | 0,038 | 25,6 | 40,2 | 0,04

The data on field gradients  $\nabla H_1$  and  $\nabla H_2$  are also shown in Figs. 16 and 17 where the moment of the first field measurement (before the flare) is taken as the zero moment. Here the values  $\nabla H_1$  and  $\nabla H_2$  are connected by a straight line only for the purpose of clearness, and not to confuse the flare. The interval in which the flare occurs is indicated by a heavy line on these straight lines. What is conspicuous in Tables 7-10 is the fact that flares with cosmic rays of intensity points 3 and 3+ are accompanied by considerably greater field gradients near the zero point than the usual flares of point 3, and especially point 2+ and 2. We can see that the flares producing cosmic rays (particularly protons) at the surface of the earth are accompanied by field gradients near the zero point which are almost twice as large as in the case of flares emitting milder cosmic rays (protons) which penetrate mostly the polar cap region, and these flares occur in field gradients which are more than twice as large as the gradients of the usual point 3 flares. As for the flares of points 2 and 2+ , the field gradients in which they usually occur are on the average four times lower than the gradient required for the usual flares of point 3 which do not generate cosmic rays. This naturally prompts the assumption that the generation of cosmic rays by the flares is closely associated with the intensity of the magnetic field in the neighborhood of the flare. Furthermore, it is very characteristic that there is not a single point 3 flare in which the field gradient near the zero point before the flare was less than 0.10 gauss/km, as there is not a single point 2 flare whose gradient exceeds 0.1 gauss/km. Attention is also called to the fact that the recurrent flares in this groups produce "a cascade reduction"

of  $\nabla H$ , as it were, near the zero point: if the first flare "lowers" the value of  $\nabla H$  to a definite level, at which a powerful flare is still possible, that level will then slightly rise and a new discharge of the intensity will occur until the gradient reaches a "safe" magnitude ( $\sim 0.1$  gauss/km) or until the group breaks up. An example of such behavior is the group in which proton flares occurred on 10 July, 14 July and 16 July 1959. Some cases (the flares of 1 April 1960, 31 August 1957 and 3 September 1957) even revealed a slight increase in the field gradient near the zero point after the first powerful flare, but they were also followed by a "discharge", a very sharp drop in the field gradient, after the second flare in the same group.

In the vast majority of cases the field gradient near the zero point before the flare was considerably larger than the gradient after the flare, that is as if the flares were associated with the destruction of the field. This difference is the more prominent, the higher the power of the flare. A similar result is obtainable also for the average speed of the changing field  $\nabla H_a/t_2-t_1$ : the greater the power of the flare the higher the absolute value of that magnitude. A summary of the average values of  $\nabla H_1$ ,  $\nabla H_2$ ,  $\nabla H_a/t_2-t_1$  for various types of flares is cited in Table 11. The data listed there, however, do not enable us to determine when the field changes occur: before, after or during the flare. If such changes occur before the flare, the magnitude of the field change should statistically be all the greater the longer the time interval between the first field measurement and the beginning of the flare. The same holds true also for the case when these changes occur

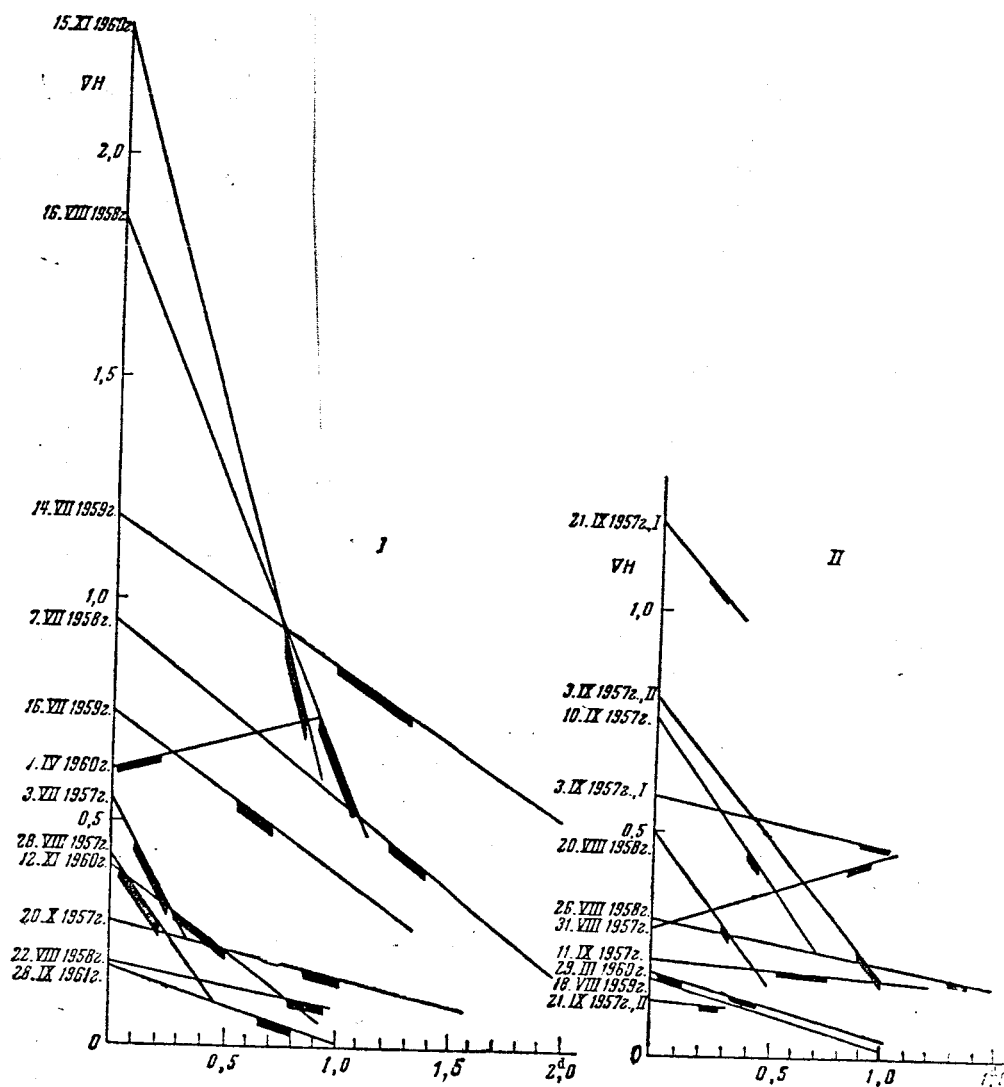


Fig. 16. A comparison of the field gradients before and after the class I and II flares

after the flare. Attempts to study the connection between  $\Delta H_a$  and the values  $t_h - t_1$  and  $t_2 - t$  have shown that there is no connection between them -- the points are scattered at random, (and  $t_h$  and  $t_k$  are the moments

of the beginning and end of the flare). At the same time, if the field change occurs during the flare, it does not have to show any statistical increase with the duration of the flare. It will continue to increase if the changes of the field will physically determine the power of the flare. The duration dependences  $\overline{\Delta H_a}$  and  $\frac{\nabla H_a}{t_2 - t_1}$  shown in Fig. 18 indicate that the capacity and duration of the flare are determined by the changing magnetic field: the greater the field change  $\nabla H_a$ , the greater the capacity and duration of the flare.

Table 11

Flare Class	Flare	No. of Cases	Field gradient Before After (gauss/km)		Speed of changing field (gauss/day)	Flare duration	Field change at zero point (gauss/day)
1	Proton flare(ball.)	13	0,78	0,27	400	>0d,17	384
2	(PCA)	11	0,45	0,27	284	>0,089	225
3	Point 3 w/o PCA	12	0,18	0,13	83	>0,071	63
4	2+ & 2, ordinary	15	0,054	0,038	40	0,048	25

That the flares are connected with the conversion of the magnetic energy of the cosmic rays to thermal energy is also indicated by the direct observation data on the field changes produced by the flares discussed at the beginning of this paragraph (Table 5 and Fig. 6). We see that the relative change in the distance between similar poles produced by  $\delta R/R$  flares is on the average  $\sim +0.32$ . The interaction energy of the poles considered as dipoles  $\sim m_1 m_2 / R^3$  thereby changes by  $\delta W = -3 \frac{m_1 m_2}{R^3} \cdot \frac{\delta R}{R}$  on the order of magnitude of the magnetic moment of the spots  $m_1 \approx m_2 = H S h \approx 10^3 (10^9)^2 h = 10^{21} h$ , where  $h$  is the length of the dipole, so that, assuming that  $h \approx R \approx 10^{10}$ , we

will get  $\delta W \approx 3 \cdot 10^{42} / 10^{10} \approx 0,3 \cdot 10^{32}$  erg, which practically coincides with the energy carried off by the cosmic rays during the flares.

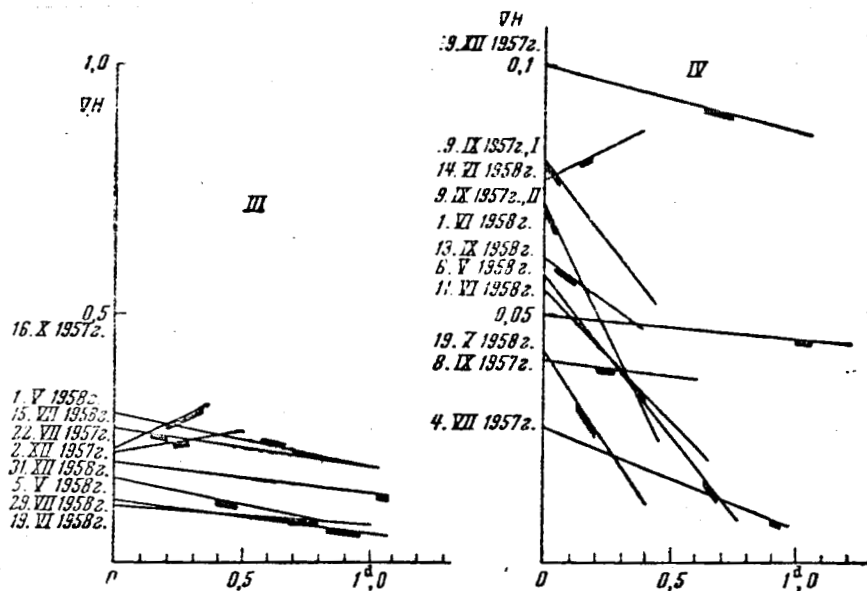


Fig. 17. A comparison of the field gradient before and after the class III and IV flares

Let us take a closer look at the field configuration accompanying proton flares (Fig. 6) and ordinary point 3 flares without geophysical effects as shown in Fig. 7. If the first case reveals real and conspicuous changes, such as the expulsion of the pole or the rearrangement of the poles, no such changes are observable in the second case, although the changes in the field intensity of the individual poles are not appreciably different from the same changes occurring in the proton flares. This suggests that the main feature of the generation of cosmic rays by the flares is not so much the field

intensity in the individual spots as their arrangement and the changes in their arrangement (this, incidentally, is quite natural if the flares occur at the zero point, as the field intensity near the zero point is proportional to the dipole moment of the spots in the first degree and the distance to the spots in minus third degree). Attention to the importance of such a reconstruction for the generation of cosmic rays was also called in [32] and [33].

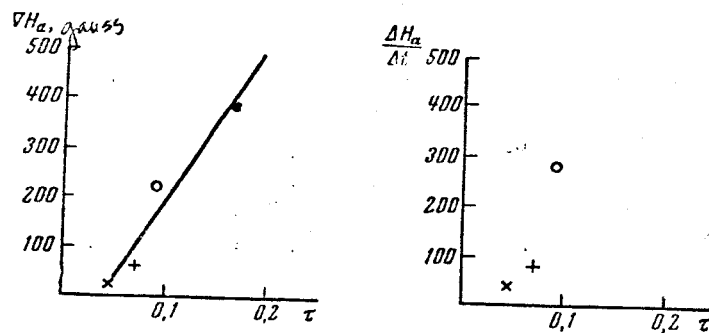


Fig. 18. The dependence of field gradient  $\nabla H_a$  near the neutral point and average (daily) field change on the duration (capacity) of the flare

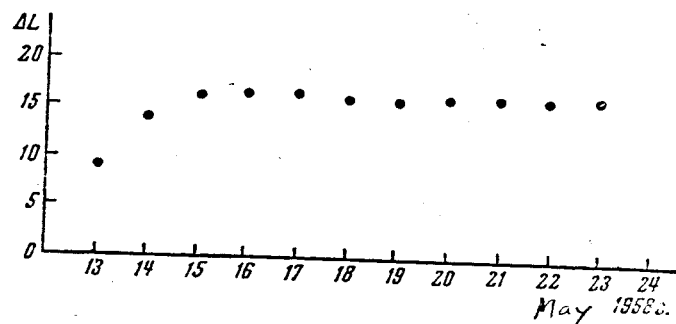


Fig. 19. The distance between the principal spots of the bipolar group 13,234 (May 1957)

Concluding this part, we will dwell briefly on a very important question (which will be discussed in detail in one of the following works): to what extent are the mentioned field changes characteristic only of flares, that is, are they possible manifestations of the usual normal development of group fields?

If we consider the groups that do not originate any flares (or originate point  $\leq 2$  flares), we will find that they include the simplest bipolar groups consisting of two spots or two subgroups arranged at some distance from one another (a distance exceeding the size of the subgroups) which changes very little if at all (see, for example, Fig. 19) increasing slightly with time, which is a well known effect. The intensity of such group components also shows very little change with time. The simplest bipolar group does not produce any flares even if the two polarities N and S are very close to each other. That is, if they come in contact in the nucleus of the same umbra; such a case, which is not uncommon, was first observed by the Mount Wilson Observatory [26]. The statement occurring in foreign literature to the effect that "flares originate at the interface of polarity" is therefore probably devoid of any meaning; see [34], for example. But a flare in a bipolar group occurs as soon as a third spot comes into being, that is as soon as a zero points originates. By the same token, flares never originate in the case of two poles of the same polarity. From the point of view of dipoles interaction, such configurations are unstable and should repel each other. Only the appearance of the third pole of opposite polarity makes possible not only a more or less lengthy existence of the configuration and zero point but also the expansion of the fields near the

zero point by drawing the poles closer or rearranging them. As for the multipolar groups, it is very difficult to study them: it is difficult to define the period when flares do not occur, and frequently impossible to identify the same spots from day to day. It is known, however, that the largest number of flares occurs when the group increases, when the number of spots, their area and the field increase. If the reduction of  $VH$  found above were not connected with the flares but expressed a normal development of a large group, it would have meant that the flares occur during the attenuation of the group, whereas actually they originate primarily when the field is increasing in magnitude and complexity. It is therefore probably that the flare occurs as a result of a growing field and that is it followed by only a temporary reduction of the field if the group has not exhausted itself. All these questions obviously call for a special study.

### 3. FLARE-PRODUCED CHANGES OF MAGNETIC FIELDS

#### (Magnetograph Data)

That the magnetic fields change during the flares can be judged from the field records made by a magnetograph [22, 23]. These records make it possible to compile charts on which the closed contours, the isogausses, are plotted across the same intensity values of the magnetic field (expressed in potentiometer subdivisions [35]). In the period of observations with a magnetograph (since 1957), the Crimean Astrophysical Observatory has made many records of magnetic fields in active regions. Some of that information has already been published as a series of magnetic field charts in [22]. These contain, in

particular, all the entries on the magnetic fields of the active group in which the famous point 3+ proton flare occurred on 22 August 1958. Only individual charts of various active regions are published in [11]. Cited below are series of entries on the magnetic field of the active solar regions discussed in paragraphs 1 and 2 which produced powerful flares and were followed by increasing intensities of the cosmic rays, namely on 14 July 1959 (Fig. 20), 15 July 1959 (Fig. 21), 16 July 1959 (Fig. 22), 17 July 1959 (Fig. 23), 18 August 1959 (Fig. 24) and, finally, 1 April 1960 (Fig. 25)\*. On the mentioned charts the zero line consists of a dotted line, and the off-scale reading regions are crosshatched. The figures on the magnetic charts of the active groups and the flares originating in them are assembled in Table 12.

Indicated in the second column of Table 12 is the number of the group (Mount Wilson)\*\*; in the third column are the days when the entries were made; in the fourth the universal time indicating the beginning of the magnetic field recording; in the fifth is the wavelength of the line in which the field entries were made; in the sixth the calibration in gauss; in the seventh the universal time of the flare, and in the eighth the intensity point of the flare.

---

\* All these charts were investigated in [23] in the study of the displacement of the magnetic "knolls" associated with the flares.

\*\* The numeration of the groups according to Mount Wilson applies only to the IGY period; the others do not have any numbers.

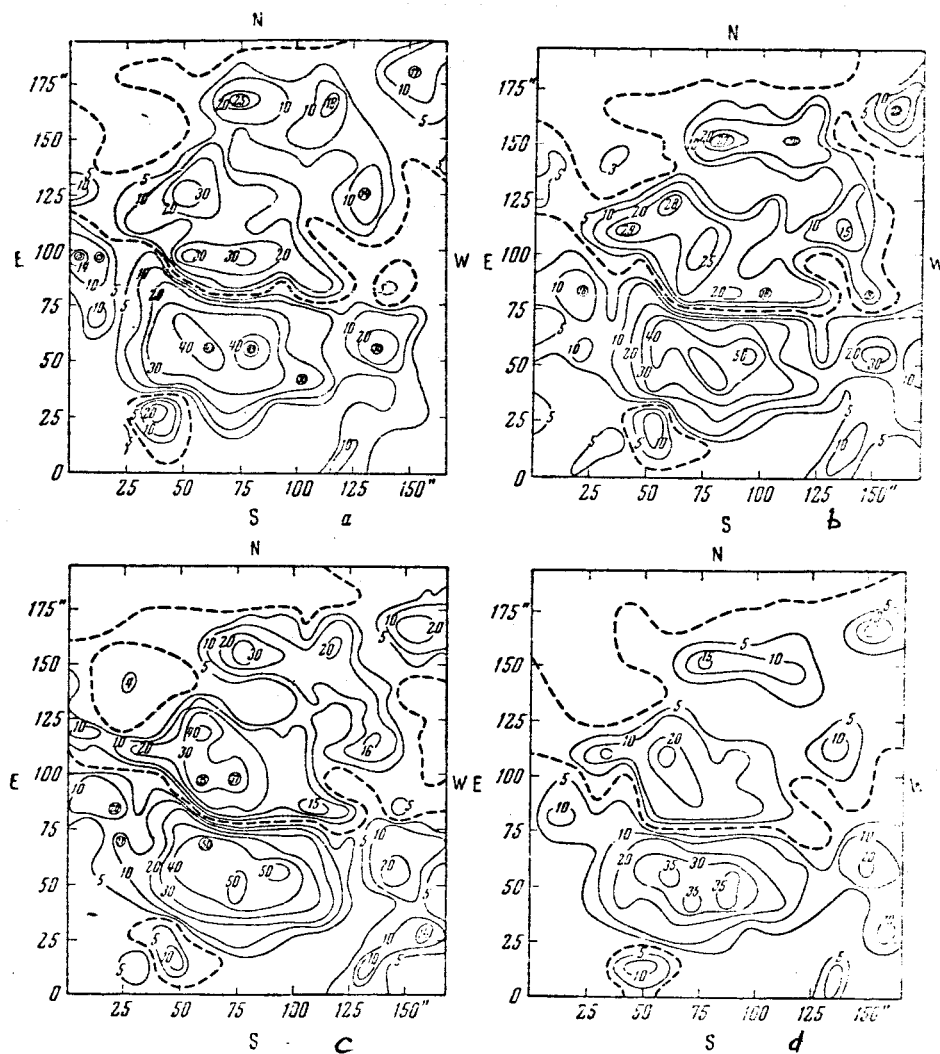


Fig. 20. Charts of the magnetic field of the active group of 14 July 1959

a-6:54 (during the point 3+ flare);  
 b-8:03 (during the point 3+ flare);  
 c-8:56 (during the point 3+ flare);  
 d-13:55 (after the point 3+ flare).

The charts of a magnetic field of the same active group are shown in Figs. 20-23.

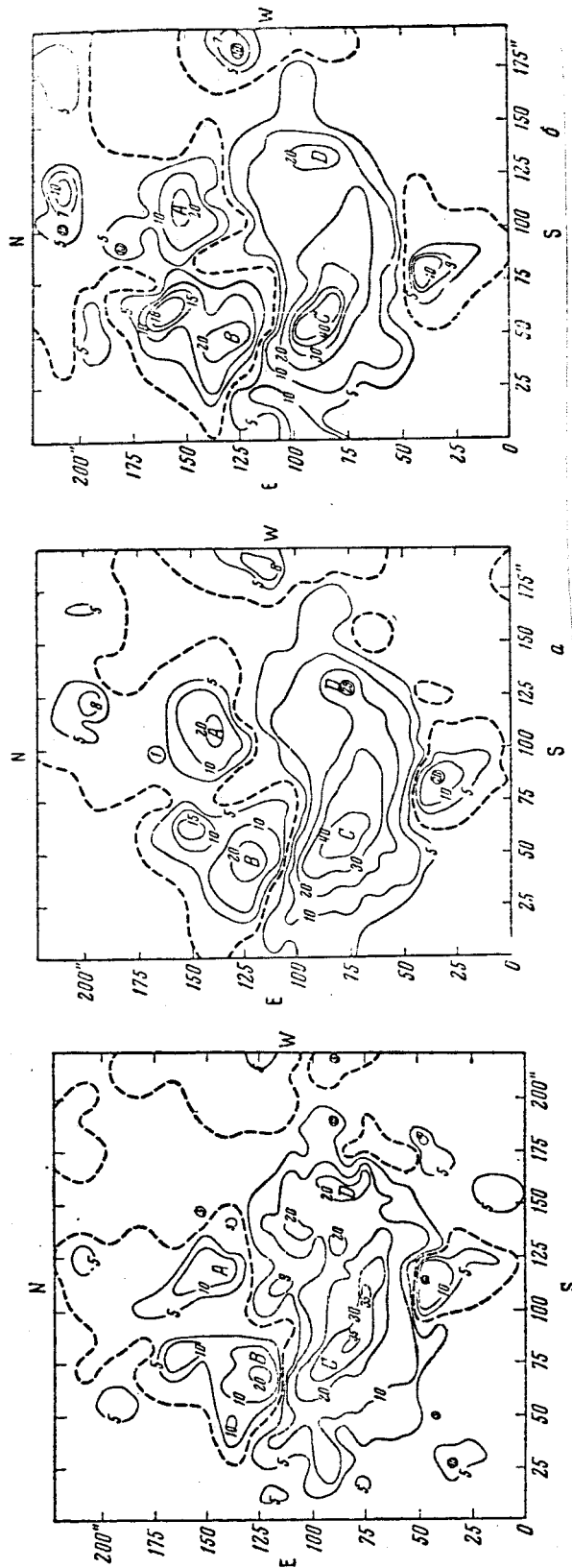


Fig. 22. Magnetic field chart of the active group of 16 July 1959.

a-11:35 (before the point 3+ flare);  
b-15:00 (before the point 3+ flare).

Fig. 21. Magnetic field chart of the active group of 15 July 1959, at 13:10

Table 12

No.	Group number	Field Recording date	Beginning of field recording Universal time	$\lambda$	One Grad. Gauss	Duration of flare Univ. time	Flare intensity	Remarks
1	12434	3.VII 1957	1,8 <sup>h</sup> 45 <sup>m</sup> — 2,10 30—	5250,2 5250,2	5,3 7,5	7 <sup>h</sup> 12 <sup>m</sup> —11 <sup>h</sup> 45 <sup>m</sup>	3+	Records made during flare
2	13464	20.VIII 1958	1,14 00—	4886,3	40,0	—	—	—
3	13464	22.VIII	1,11 50— 2,14 20— 3,15 00—	4886,3 4886,3 4886,3	18,3 24,4 37,0	13 17—14 05 — 14 17—17 17 $\Delta$	2+  3	Before the flare After flare Beginning of flare
4	13464	23.VIII	1,12 50—	4886,3	25,0	—	—	After flare
5		14.VII 1959 *	1,6 54— 2,8 03— 3,8 56— 4,13 55—	4886,3 4886,3 4886,3 4886,3	13,6 16,4 13,4 37,6	3 25E—11 21	3+	During flare Ditto "
6		15.VII	1,13 10—	4886,3	29,2			After the flare
7		16.VII	1,11 35— 2,15 00—	4886,3 4886,3	16,5 26,3			Before flare
8		17.VII	1,6 00—	4886,3	8,7	21 14—24 30	3+	Ditto After flare
9		18.VIII 1959	1,7 45— 2,13 45—	4886,3 4886,3	18,0 14,0	10 19—12 50	3	Before flare After flare
10		1.IV 1960	1,10 15— 2,11 20— 3,14 05—	4886,3 4886,3 4886,3	39,0 23,4 35,0	8 40—13 20	3+	After max. flare At end of flare After flare

\* The same active region was recorded between 14 and 17 July 1959.

All the figures in Table 12 may be divided into two groups. The first group includes the recordings made during the flare (3 July 1957, 14

July 1959 and 1 April 1960). The second group includes the flares for which there is at least one entry made before the beginning of the flare and after its end. The entries on the magnetic field after the point 3+ flares of 22 August 1958 and 16 July 1959 were made on 23 August 1958 and 17 July 1959 respectively. (See Table 12). In the first case the time interval between the two successive entries is 22 hours, and in the second case 15 hours. In both of these cases, however, the active regions were not very far from the central meridian (see Table 1) where the effect of the changing projection on the changing intensity of the magnetic field is probably not very substantial. It may therefore be assumed that the changes in the distribution of the magnetic field in these cases are due to the flare processes.

The information received on 18 August 1959 (see Fig. 24) is unique. The point 3 flare began at 10:19 and ended at 12:50. The first entry on the magnetic field in this region was made 2.5 hours before the beginning of the flare. Measurements were repeated made one hour after the end of the flare (see Table 12). The interval between these two measurements of the magnetic field was about 6 hours. We are therefore justified in saying that the difference in the distribution of the magnetic field on both charts are due to the flare (see Fig. 24).

The changes of the magnetic field can be estimated by the diminution or growth of its gradients. The magnetic field charts shown in Figs. 22-25 as well as those published in [22] and [11] were used in order to find the intensity gradients of the magnetic field and their changes associated with the flares. Inasmuch as the charts published in [22] and [11] do not contain the designations

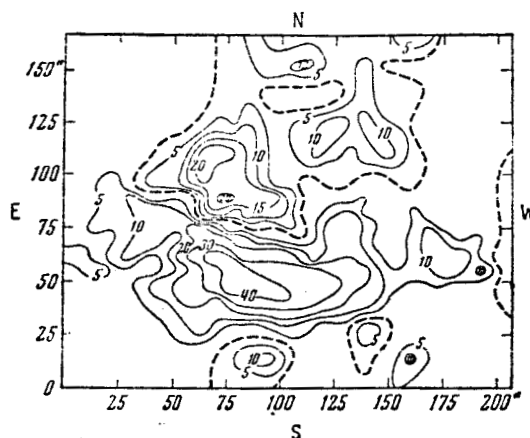


Fig. 23. Magnetic field chart of the active group of 17 July 1959

at 6:00 (after the point 3+ flare)

we are using here, we will reproduce one chart for 3 July 1957 (Fig. 26) and one for 22 August 1958 (Fig. 27)/ The most characteristic configuration of the magnetic field "knolls" which was identified in all the other records of the same group was selected on the basis of these charts as well as those published in [22] and [11]. The centers of the magnetic field "knolls" were connected with straight lines. Measured along these straight lines were the magnetic field intensities at different distances from the center of one of the "knolls"; the center of that "knoll" was indicated by the first letter in the designations of the corresponding directions (A - B, C - D, etc.). The results of the measurements are cited in Fig. 28 where the intensity of the longitudinal magnetic field is measured off in gauss along the Y-axis, and the distance in kilometers along the X-axis. Straight lines were then drawn through the resulting points. The incline of these straight lines represents the magnetic field gradient. Inasmuch as the straight lines are drawn through a large number of points, it may be assumed that the gradient has been de-

terminated fairly reliably. The values of the gradients are listed in Table 13.

A look at the data in Table 13 shows that in the case of the first group, the gradients are decreasing in some directions and increasing in others. And the decrease of the gradients in one direction is not substantially different from their increase in another direction. As a result, it may be said that the first group of entries does not show any very tangible reduction of the gradients. Here it should be borne in mind that in the event of 3 July 1957 both measurements were during the flare, and the result cannot therefore be compared to the one following from the examination of the field configuration in Part Two where the data on the absolute field before and after the flare were used. As for the event of 1 April 1960, the results shown in Table 13 practically agree with the data of Part 2.

As for the second and more numerous group of cases, it is possible to determine the direction of the gradient changes before and after the flare. Here we can see the following fairly characteristic picture of changing gradients: before the flare and toward its beginning the field gradient reveals an appreciable increase in most directions (compare the data for 20 August 1958 and 22 August 1958 before the point 2+ flare and after that flare as well as the data for the beginning of the point 3+ flare in the same day; also the gradients before the point 3+ flare of 16 July 1959). After the flare, the gradients show an appreciable decrease in most directions (compare gradient  $\nabla H$  for 22 August 1958 at 15:00 and 23 August 1958 at 12:50, for 16 July 1959 at 15:00 and 17 July 1959 at 6:00, as well as the event of

GROUP I

Table 13

Date	Beginning of recording UT	$\nabla H \cdot 10^2$ (For measurement direction) gauss/km								Remarks		
		A-D <sub>I</sub>	A-D <sub>II</sub>	C-D <sub>I</sub>	C-D <sub>II</sub>	C-D <sub>III</sub>	C-D <sub>IV</sub>	A-C <sub>I</sub>	A-C <sub>II</sub>			
3.VII. 1957	8 <sup>h</sup> 45 <sup>m</sup>	2,5	2,5	4,6	4,6	2,7	2,7	7,5	5,0	During point 3+ flare		
	10 30	2,5	2,5	4,3	4,3	3,0	3,0	8,6	3,7	Ditto		
		C-B <sub>I</sub>	C-B <sub>II</sub>	E-D <sub>I</sub>	E-D <sub>II</sub>	E-A <sub>I</sub>	E-A <sub>II</sub>					
1.IV 1960	10 <sup>h</sup> 15 <sup>m</sup>	7,4	22,0	15,4	11,0	7,7	5,9			During point 3+ flare		
	11 20	6,2	12,5	8,7	16,7	7,7	5,9			Ditto		
	14 05	7,7	16,7	9,1	11,8	4,9	5,9			After point 3+ flare		
GROUP II												
		C-G <sub>I</sub>	C-G <sub>II</sub>	A-C <sub>I</sub>	A-C <sub>II</sub>	C-D <sub>I</sub>	C-D <sub>II</sub>	E-C <sub>I</sub>	E-C <sub>II</sub>	A-B <sub>I</sub>	A-B <sub>II</sub>	
20.VIII 1958	14 <sup>h</sup> 00	7,2	7,2	12,5	12,5	—	—	—	—	—	—	
22.VIII	11 50	11,1	11,1	3,7	40,0	10,0	2,5	9,1	10,0	12,5	12,5	Before point 2+ flare
	14 20	8,3	8,3	5,3	10,0	10,0	10,0	7,4	7,4	25,0	12,5	After point 2+ flare
	15 00	14,3	14,3	20,0	20,0	13,6	13,6	10,5	16,7	—	—	At beginning of point 3+ flare
23.VIII	12 50	8,0	8,0	10,0	10,0	13,4	5,0	11,0	16,7	—	—	After point 3+ flare
		B-A <sub>I</sub>	B-A <sub>II</sub>	C-D <sub>I</sub>	C-D <sub>II</sub>	B-C <sub>I</sub>	B-C <sub>II</sub>	A-D <sub>I</sub>	A-D <sub>II</sub>			
16.VII 1959	11 <sup>h</sup> 35 <sup>m</sup>	1,8	2,3	1,1	3,0	7,4	7,4	2,5	2,0			Before point 3+ flare
17.VII	15 00	3,3	2,4	2,0	3,5	9,0	9,0	6,5	2,0			Ditto
	6 00	1,2	1,2	0,38	0,5	2,25	2,25	1,0	0,5			After point 3+ flare
		A-B <sub>I</sub>	A-B <sub>II</sub>	B-C <sub>I</sub>	B-C <sub>II</sub>	A-D <sub>I</sub>	A-D <sub>II</sub>	B-D <sub>I</sub>	B-D <sub>II</sub>	B-D <sub>III</sub>	B-D <sub>IV</sub>	
18.VIII 1959	7 <sup>h</sup> 45 <sup>m</sup>	17,7	7,7	11,7	9,5	20,0	25,0	9,5	14,3	14,3	12,2	Before point 3 flare
	13 45	11,1	14,3	8,0	11,7	20,0	11,1	11,8	11,8	15,4	7,4	After point 3 flare

\* I, II, III and IV indicate which part of the curve is used in Fig. 28.

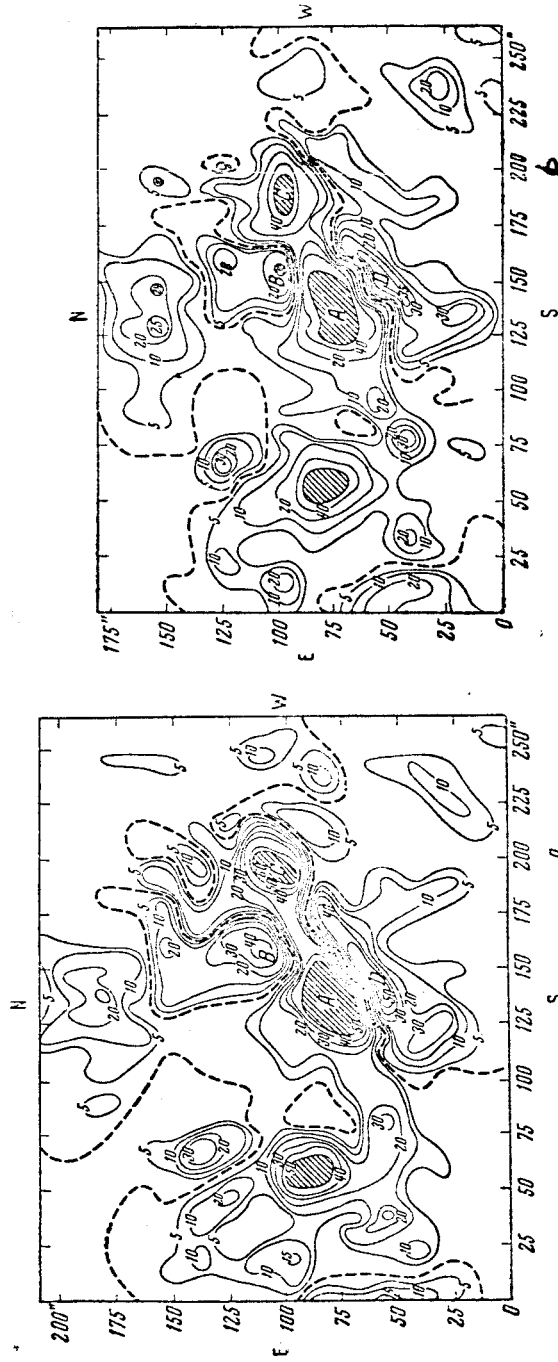


Fig. 24. Magnetic field charts of the active group of 18 August 1959

a- 7:45 (before the point 3 flare);  
b-13:45 (after the point 3 flare).

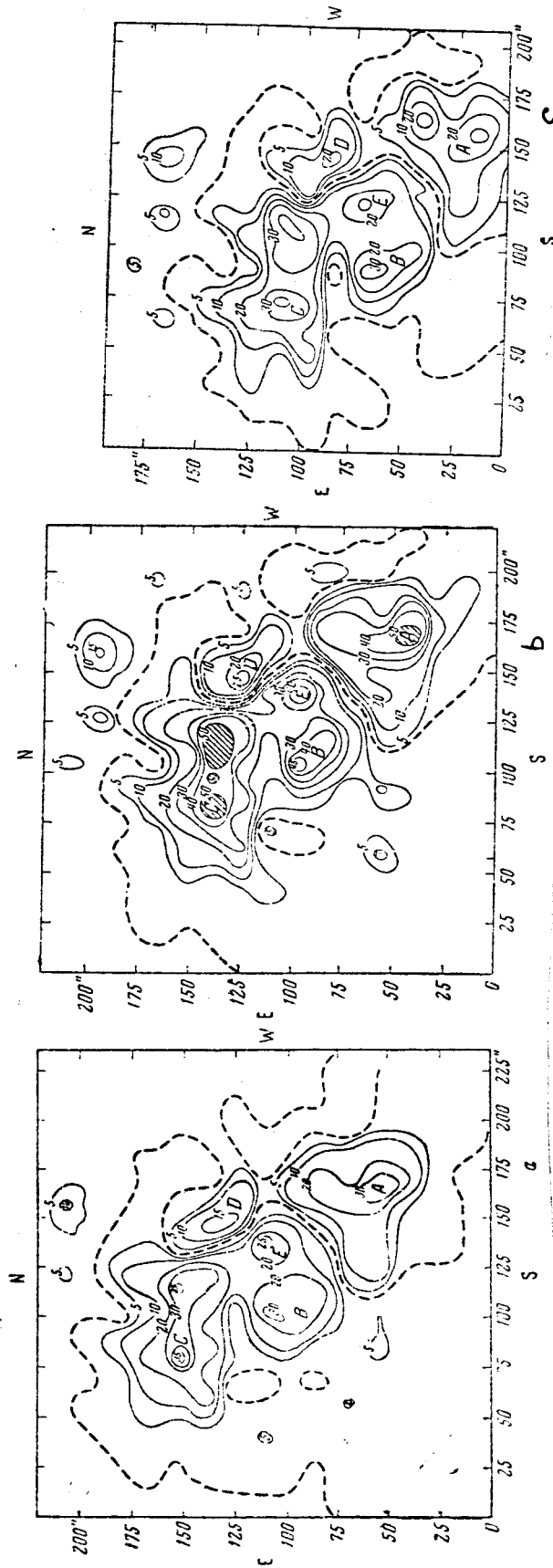


Fig. 25. Magnetic field charts of the active group of 1 April 1960.

a-10:15 (after maximum flare of point 3+);  
 b-11:20 (at end of point 3+ flare);  
 c-14:05 (after point 3+ flare).

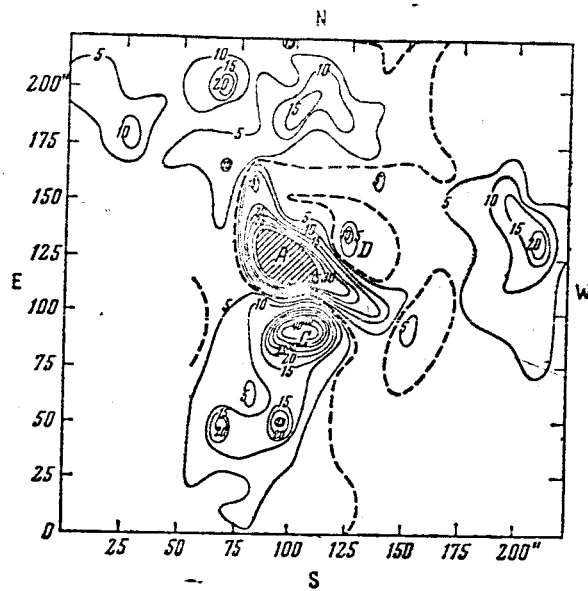


Fig. 26. Magnetic field chart of active group 12,434 of 3 July 1957 at 10:30 (at the end of the point 3+ flare)

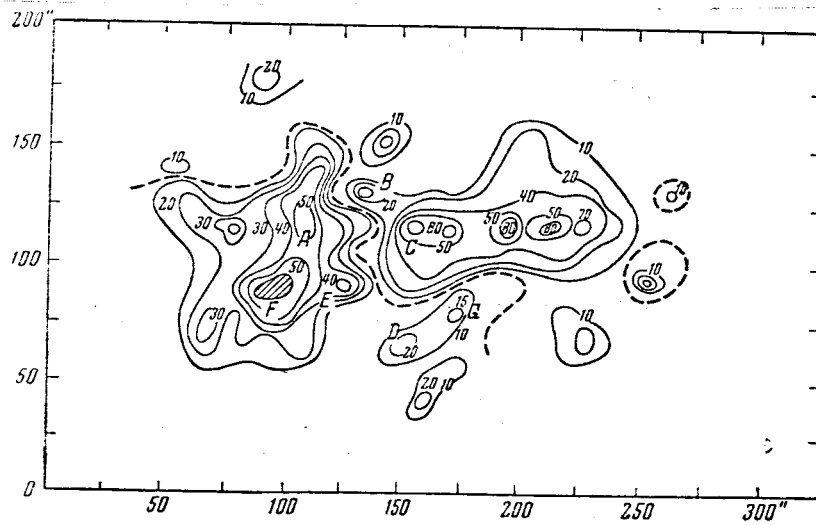


Fig. 27. Magnetic field chart of active group 13,464 of 22 August 1958 at 11:50 (before point 2+ flare)

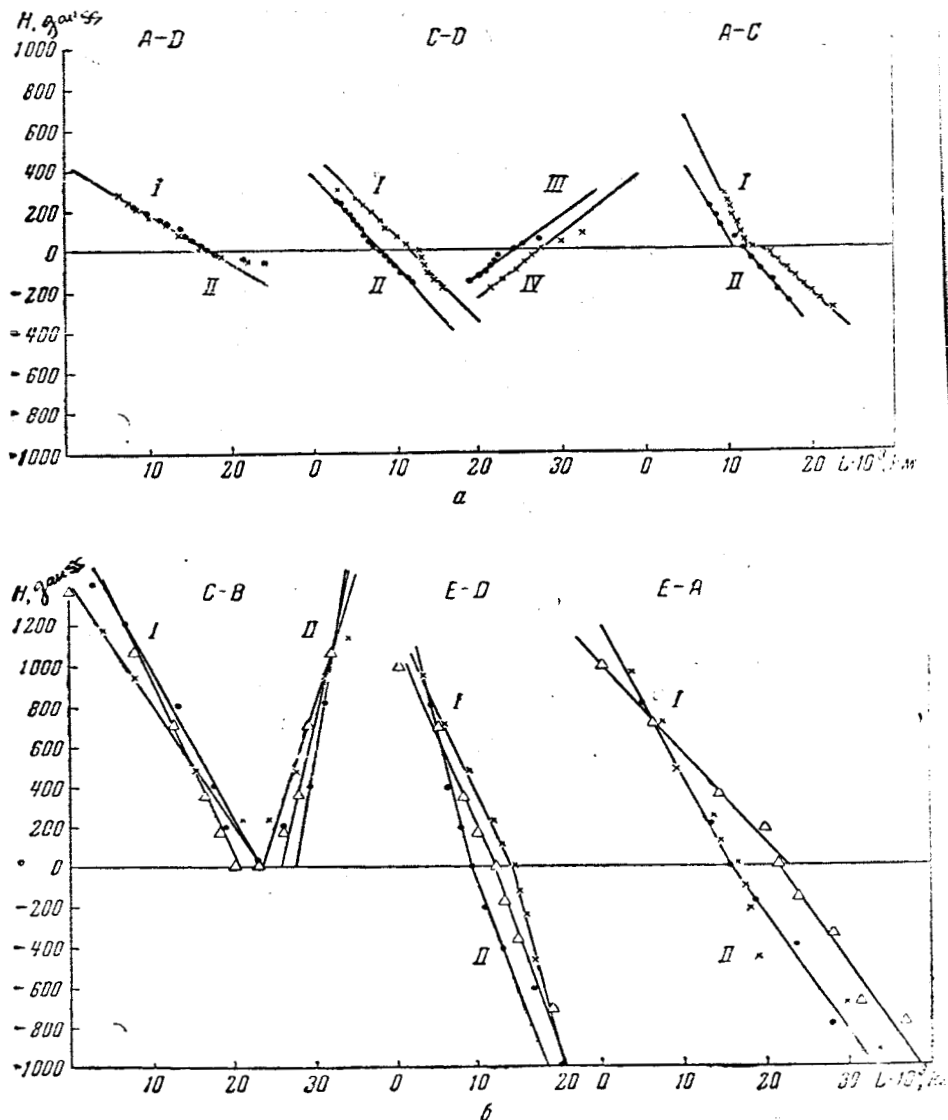


Fig. 28. Changing magnetic field in the most characteristic direction in the active groups (see also pp. 78 and 79 of text)

a-3 July 1957: points--8:45 (during point 3+ flare), crosses-- 10:30 (during point 3+ flare); b-1 April 1960: points--10:15 (after maximum of point 3+ flares), crosses--11:20 (at the end of point 3+ flare), triangles--14:05 (after point 3+ flare); c-20 July 1958: squares--14:00, 22 August 1958: circles--15:00 (at the beginning of point 3+ flare), 23 August 1958: triangles--12:50 (after point 3+ flare); d-22 August 1958: points--11:50 (before point 2+ flare), crosses--14:20 (after point 2+ flare), circles--15:00 (at the beginning of point 3+ flare); e-16 July 1959: points--11:35 (before point 3+ flare), 16 July 1959: circles--15:00 (before point 3+ flare), 17 July 1959: 6:00 (after point 3 flare); f-18 August 1959: points--7:45 (before point 3 flare), crosses--13:45 (after point 3 flare).

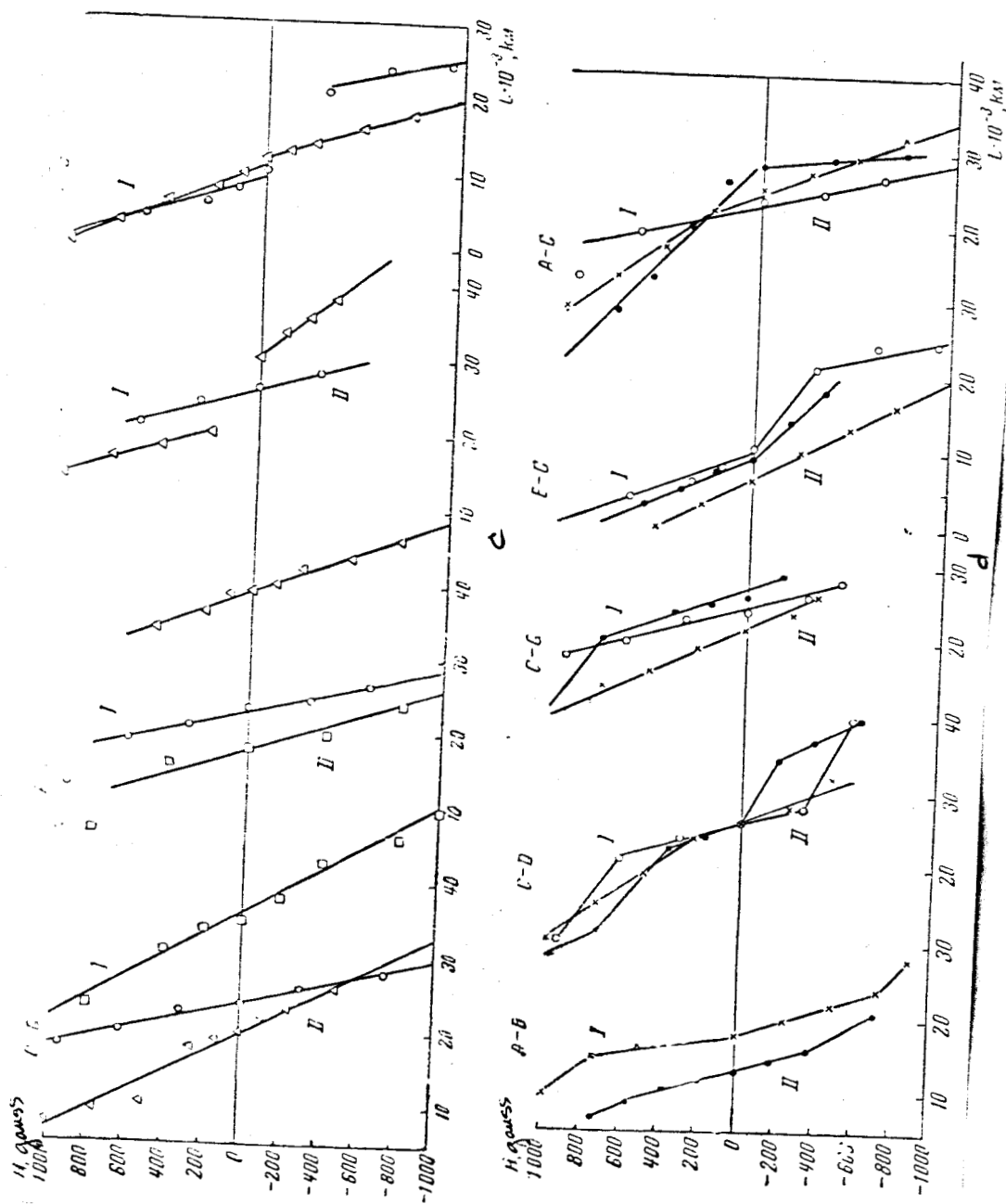


Fig. 28. Continued

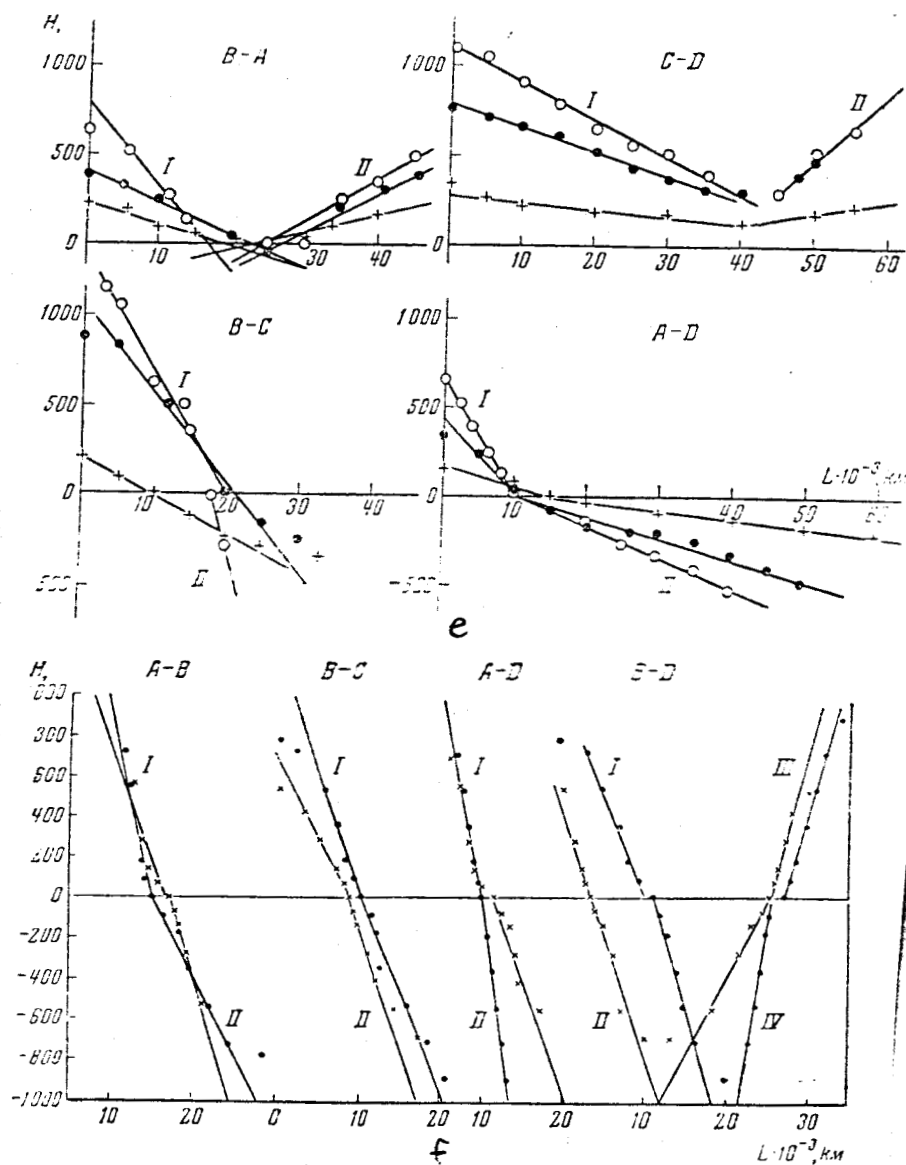


Fig. 28. End

18 August 1959), although in some directions there was a slight increase in  $\Delta H$  which was considerably smaller than the increase in other directions. Qualitatively, this result agrees with the one obtained in Part 2; but a

quantitative comparison in this case is not fully justified as Part 2 deals with the gradient of the transverse field near the zero point whereas in this case we are measuring the gradient of the longitudinal field in the direction of the straight line connecting the individual poles. However, in the case of the flares of 22 August 1958, for example, the  $\nabla H$  in both cases practically coincide (here the gradient is 0.10-0.20 gauss/km, and there the gradient was found to be 0.18 gauss/km). Here the  $\nabla H$  of the flare of 16 July 1959 is half the size of that shown in Table 7; the gradients of the flare of 18 August 1959, listed in Table 13, practically coincide with the gradient shown in Table 8. Although the available information is still inadequate for a definite conclusion, the fact that the  $\nabla H$  increases before the flare is a matter of great interest. A similar decrease of the gradients after the flare was found also in [36], although on the day after the flare the field was back to its initial "preflare" state.

In conclusion we express our gratitude to N. V. Codovnikov, A. N. Babin and T. P. Khromova for their assistance in the calculations, and to A. E. Balkov for the preparation of the illustrations.

15 March 1962.

BIBLIOGRAPHY

1. A. B. Severnyy and Ye. F. Shaposhnikov. *Izv. Krymskoy astrofiz. obs.* [News of the Crimean Astrophysical Observatory], 12, 3, 1954.
2. H. W. Dodson and E. R. Hedeman. *IGY Solar Activity Report Series*, No. 12, 1960; N 15, 1961.
3. *Quart. Bull. Solar Activity of the I. A. U.*, N 119-128, 1957-1960.
4. *World Data Center. "A Solar Activity"*, Boulder. N 13-15, 1957-1961.
5. "Map of the Sun 1957-61". *Fraunhofer Institut*.
6. V. E. Stepanov, E. F. Shaposhnikova and N. N. Petrova. "The catalogue of strengths and polarities of magnetic fields of sunspots for the period of IGY (1 July 1957 - 31 Dec. 1958)". London, Pergamon Press (being printed).
7. A. S. Dvoryashin. *Izv. Krymskoy astrofiz. obs.* 28, 305, 1962.
8. A. S. Dvoryashin, L. S. Levitskiy and A. K. Pankratov. *Izv. Krymskoy astrofiz. obs.* 26, 90, 1961.
9. A. N. Charakhach'yan and T. N. Charakhch'yan. *Geomagnetizm i aeronomiya*. [Geomagnetism and aeronomy], 2, No. 5, 829, 1962.
10. Ye. F. Shaposhnikova and M. B. Ogir'. *Izv. Krymskoy astrofiz. obs.*, 21, 112, 1959.
11. S. I. Gopasyuk. *Izv. Krymskoy astrofiz. obs.*, 25, 114, 1961.
12. M. C. Ballario. *Mem. Soc. Astron. Italiana*, 29, N 1, 1958.
13. M. D'Azambuja, G. Olivier, J. Rayrole. *Astronomie*, Sept. 1957.
14. S. I. Abramenko, E. Ye. Dubov, M. B. Ogir', N. Ye. Steshenko, Ye. F. Shaposhnikova and T. T. Tsan. *Izv. Krymskoy astrofiz. obs.*, 23, 341, 1960.
15. B. M. Vladimirskiy, A. S. Dvoryashin, N. N. Yerushev, I. G. Moyseyev, Yu. I. Neshpor, M. B. Ogir' and N. N. Odintsova. *Izv. Krymskoy astrofiz. obs.*, 26, 74, 1961.
16. M. B. Ogir' and N. Ye. Steshenko. *Izv. Krymskoy astrofiz. obs.*, 25, 134, 1961.

17. B. Valnicek. Bull. Astron. Inst. Czech., 12, N 6, 1961.
18. R. Howard and H. W. Babcock. Astrophys. J., 132, N 1, 918, 1960.
19. M. A. Ellison, S. M. P. McKenna and J. H. Reid. Dunsink Observ. Publ. 1, No. 3, 1961.
20. M. Waldmeier. Z. Astrophys., 52, 1, 1961.
21. A. B. Severnyy. Astron. zh. [Astronomical Journal], 34, 328, 1957; Dokl. AN SSSR [Transactions of the USSR Academy of Sciences], 121, No. 5, 1958.
22. A. B. Severnyy. Astron. zh., 35, 335, 1958; Izv. Krymskoy astrofiz. obs., 20, 22, 1958; 22, 12, 1960.
23. S. I. Gopasyuk. Astron. zh., 38, 209, 1961.
24. A. Antalova. Bull. Astron. Inst. Czech., 12, N 3, 1961.
25. V. Bumba. Izv. Krymskoy astrofiz. obs., 23, 212, 1960.
26. G. Hale, F. Ellerman, S. Nicolson and A. Joy, Astrophys. J., 49, 153, 1919.
27. T. Cowling. Monthly Notices Roy. Astron. Soc., 106, N 3, 218, 1946.
28. A. B. Severnyy. Astron. zh., 36, No. 2, 208, 1959.
29. V. Ye. Stepanov and S. I. Gopasyuk. Izv. Krymskoy astrofiz. obs., 28, 194, 1962.
30. See T. Cowling. In collected works "Solntse" ["Sun"] edited by Coyper. IL [Publishing House of Foreign Literature], pp. 460-471.
31. V. Ye. Stepanov and A. B. Severnyy. Izv. Krymskoy astrofiz. obs., 28, 166, 1962.
32. A. B. Severnyy and V. P. Shabanskiy. Izv. Krymskoy astrofiz. obs., 25, 88, 1961.
33. S. I. Gopasyuk. Izv. Krymskoy astrofiz. obs., 27, 110, 1962.
34. V. Bumba. Izv. Krymskoy astrofiz. obs., 19, 105, 1958.
35. N. S. Nikulin, A. B. Severnyy and V. Ye. Stepanov. Izv. Krymskoy astrofiz. obs., 19, 3, 1958.
36. R. Michard, Z. Mouradian and M. Semel. Ann. astrophys., 24, N 1, 1961.